DALTON
PERSPECTIVE

Mechanism of the low-energy fluxional process in $[Fe_3(CO)_{12-n}L_n]$ (n = 0–2): a perspective†

Brian E. Mann*

Department of Chemistry, The University of Sheffield, Sheffield S3 7HF, UK

The methods of Bürgi and Dunitz, using crystal structures to map out an exchange pathway for the carbonyls, have been applied to $[Fe_3(CO)_{12}]$ and its derivatives. It has been shown that the exchange pathway follows that predicted by the concerted bridge-opening and bridge-closing mechanism. The data are inconsistent with other proposed mechanisms. It has also been shown that the concerted bridge-opening and bridge-closing mechanism can equally be described as a rotation of either the Fe_3 triangle or the carbonyl icosahedron about a S_{10} axis of the icosahedron through the equatorial ligands. This mechanism has been used to explain the lowest-energy fluxional mechanism in $[Fe_3(CO)_{12}]$, both in solution and in the solid state, in $[Fe_3(CO)_{11}L]$ [L = PMe_2Ph, $P(OR)_3$, $CNBu^t$, $CNCF_3$] in solution, in $[Fe_3(CO)_{10}L_2]$ [L = $P(OR)_3$ (R = Me, Et or Pr^i)] in solution and in $[Fe_2Os(CO)_{12}]$ in the solid state. The other mechanisms examined are the C_2 libration mechanism due to Johnson, the rotation of either the Fe_3 triangle or the carbonyl icosahedron about a S_{10} axis of the icosahedron through a bridging ligand and an axial ligand on the unbridged iron due to Lentz, and the 60° rotation about the C_3 axis of the Fe_3 triangle due to Hanson. It is argued that the Ligand Polyhedral Model, albeit very elegant, is misleading and has led to improbable mechanisms. The approach using the original Local Bonding Model is recommended.

The structure and spectra of $[Fe_3(CO)_{12}]$ have presented problems since its discovery in 1906.[1] It has had a long history of erroneous structures and these have been reviewed.[2] The crystal structure is now established,[3,4] but there is still considerable confusion concerning the IR and NMR spectra. The IR spectrum of $[Fe_3(CO)_{12}]$ in solution shows two strong, well defined, bands in the terminal stretching region.[5,6] The interpretation of the IR spectrum is controversial with suggestions that the weak bands are overtones/combinations,[6] are weak as the compound exists as a mixture of bridged and unbridged forms,[7] or are broadened by rapid exchange.[8] The ^{13}C NMR spectrum of $[Fe_3(CO)_{12}]$ in solution is a singlet at −150 °C,[9] but a limiting low-temperature ^{13}C NMR spectrum is observed in the solid state at −93 °C. In order to explain the fluxionality, five separate mechanisms have been proposed, the merry-go-round mechanism,[9] the concerted bridge-opening bridge-closing mechanism,[10] the C_2 libration mechanism,[11] a C_3 rotation mechanism[12] and the rotation of either the Fe_3 triangle or the carbonyl icosahedron about a S_{10} axis of the icosahedron through a bridging ligand and an axial ligand on the unbridged iron.[13] In 1992, Li and Jug[14] applied the semi-empirical SINDO1 method to $[Fe_3(CO)_{12}]$, and compared the fluxionality arising from the merry-go-round mechanism,[15] the C_2 libration mechanism,[11] and the C_3 rotation mechanism,[12] in the solid state. They concluded that of these three mechanisms, the merry-go-round mechanism is most probable in solution, while the C_2 libration mechanism is most probable in the solid state. Recently Sironi[16] has used molecular mechanics calculations and produced results which are in agreement with the C_2 libration mechanism. Unfortunately, neither the concerted bridge-opening bridge-closing mechanism nor the C_5 rotation mechanism was considered in either of these theoretical papers. In this paper the proposed mechanisms for the low-energy fluxionality of ligands in $[Fe_3(CO)_{12}]$ and its derivatives are examined.

In 1966, Cotton[9] proposed the merry-go-round mechanism of carbonyl scrambling for $[Co_4(CO)_{12}]$ fluxionality. The ^{13}C NMR spectrum of $[Fe_3(CO)_{12}]$ at −150 °C is a singlet, with $\Delta G^{\ddagger} < 25$ kJ mol^{-1}. The fluxional mechanism involves exchange between isomers with bridging and terminal carbonyl groups. In the case of $[Fe_3(CO)_{12}]$, this involves exchange between the bridged, **1**, and terminal, **2**, forms, see Scheme 1.[3,15] The Local Bonding Model was used to describe the exchange. (There are two methods of describing metal clusters. One uses local bonds and produces structures such as those in Scheme 1. This will be referred to as the Local Bonding Model. The alternative representation views the ligands as a polyhedron, and is referred to as the Ligand Polyhedral Model.[17]) Strong support for the merry-go-round mechanism came from an analysis by Crabtree and Lavin[18] of the crystal structures of a number of iron compounds using the Bürgi–Dunitz approach.[19]

In 1966, Wei and Dahl and, independently, Corradini and Paiaro[20] realised that the carbonyls of $[Fe_3(CO)_{12}]$ and $[Co_4(CO)_{12}]$ form a relatively close-packed distorted icosahedron.[2] Subsequently, in 1978, Benfield and Johnson[17] developed this into the Ligand Polyhedral Model. They proposed a fluxional mechanism involving an icosahedron↔cube-octahedron↔icosahedron rearrangement of the carbonyl ligands.[21] Five modes of ligand scrambling were identified, two pairs of which are identical for $[Fe_3(CO)_{11}\{P(OMe)_3\}]$, see Scheme 2.

Johnson and co-workers[21] had already shown that, at −90 °C, $[Fe_3(CO)_{11}\{P(OEt)_3\}]$ **3** [L^1, L^2 = CO, $P(OEt)_3$] shows three carbonyl signals, which they believed to have the intensity ratio 6:4:1 at δ 221.9, 219.0 and 204.6. None of the modes in Scheme 2 gave this intensity ratio. Mode C came closest giving intensities 4:4:2:1, with the other modes giving 8:1:1:1. They concluded that there are two very low energy dynamic processes operating at −90 °C, mode C, and a trigonal twist at the unsubstituted iron with bridging carbonyls. This would result in the exchanging sets of carbonyls being C^3O, C^4O, C^6O, $C^{10}O$, $C^{11}O$ and $C^{12}O$; C^1O, C^2O, C^8O and C^9O; and C^5O. This mechanism was unlikely on the basis of the experimental results then available. The signal for carbonyls, C^1O, C^2O, C^8O and C^9O, should come halfway between the bridging region, δ 250–280, and the terminal region, δ 200–220, yet was actually at δ 219.[22] The situation is even worse for $[Fe(CO)_{11}(PMe_2Ph)]$, where the signal of intensity '4' comes at δ 212.3.[21]

* E-Mail:b.mann@sheffield.ac.uk

† A web movie has been made of the rotation of the carbonyls around the S_{10} axis and can be found at http://chemistry.rsc.org/rsc/fe3-carb.htm. This movie will be available *via* the RSC web server until 1st January 2000, after which details may be obtained from Professor Mann.

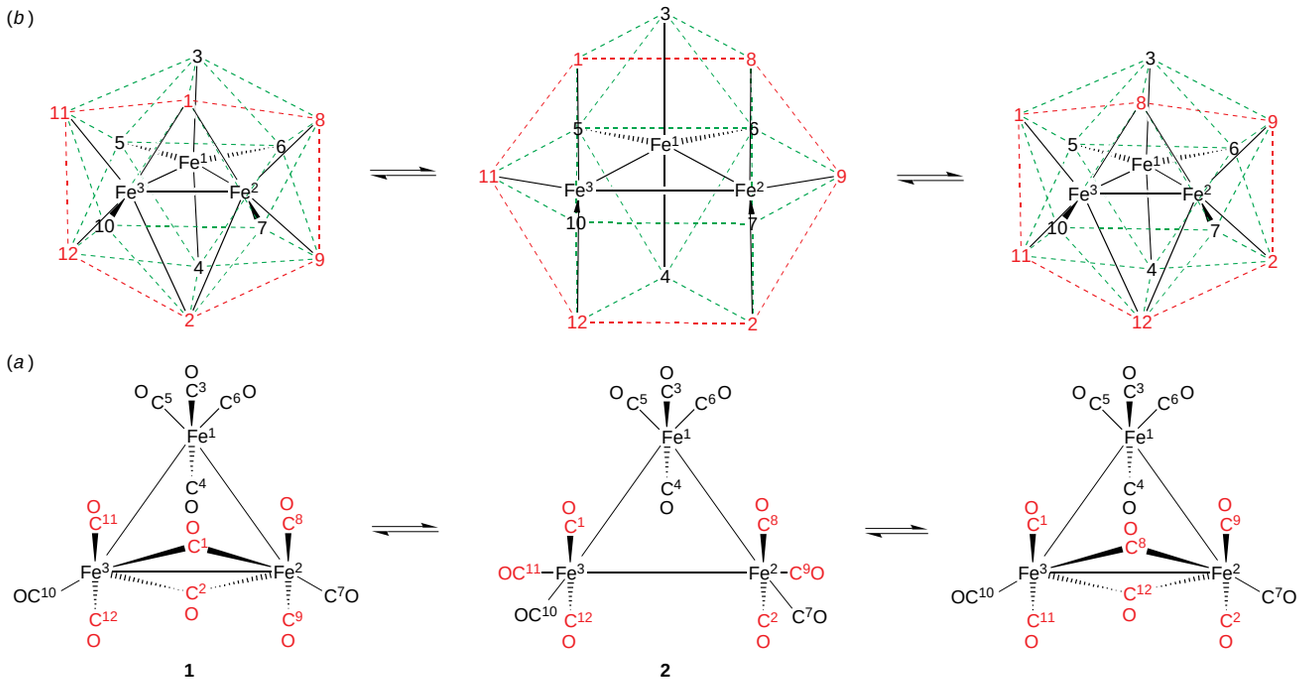

Scheme 1 The Cotton merry-go-round mechanism is applied to $[Fe_3(CO)_{12}]$ **1** with the carbonyls represented by numbers. The mechanism shown exchanges the carbonyls $C^{1}O{\leftrightarrow}C^{11}O{\leftrightarrow}C^{12}O{\leftrightarrow}C^{2}O{\leftrightarrow}C^{9}O{\leftrightarrow}C^{8}O$. Exchange of the other carbonyls is achieved by bridge closure about the other Fe–Fe edges. (*a*) The mechanism is represented using the Local Bonding Model. (*b*) The mechanism is represented using the Ligand Polyhedral Model, with the carbonyls represented by numbers

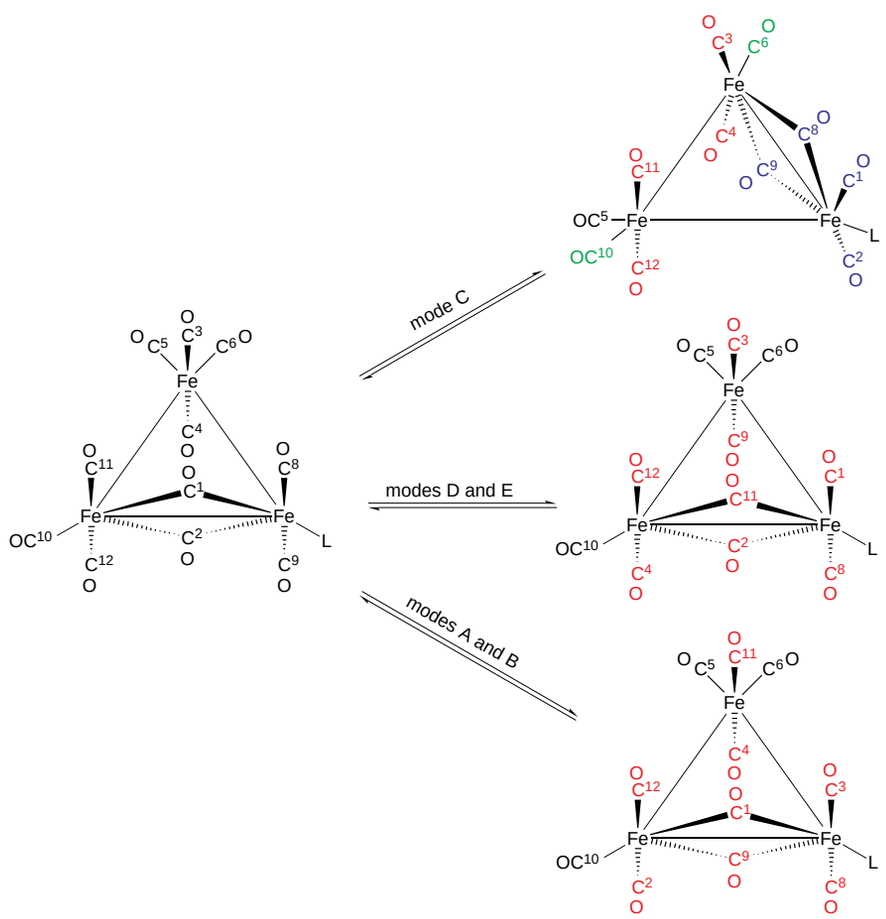

Scheme 2 The ligand exchange predicted by the Ligand Polyhedral Model, as applied to $[Fe_3(CO)_{11}L]$, where L = a phosphite ligand, based on the original icosahedron↔cube-octahedron↔icosahedron rearrangement.[21] In the structures on the right, the same colour is used for an exchanging set of carbonyls. Black is used for unique carbonyls

In 1987, Farrar and Lunniss[23] examined the fluxional behaviour of $[Fe_3(CO)_{10}\{P(OMe)_3\}_2]$ and $[Fe_3(CO)_{10}\{P(OMe)_3\}\{P(OPh)_3\}]$. They concluded that, in solution, $[Fe_3(CO)_{10}\{P(OMe)_3\}_2]$ consists of two isomers, **3** $[L^1 = L^2 = P(OMe)_3]$ or **4** $[L^1 = L^2 = P(OMe)_3]$ and **5** $[L^1 = L^2 = P(OMe)_3]$. They also concluded that at −80 °C for **3** or **4** there is a rapid merry-go-

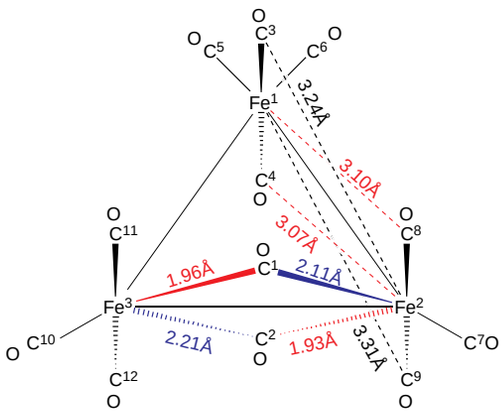

Fig. 1 The complex $[Fe_3(CO)_{12}]$ showing key Fe–C distances relevant to the concerted-bridge-opening bridge-closing mechanism.[10] Bonds which are forming or strengthening are shown in red. Bonds which are breaking are shown in blue

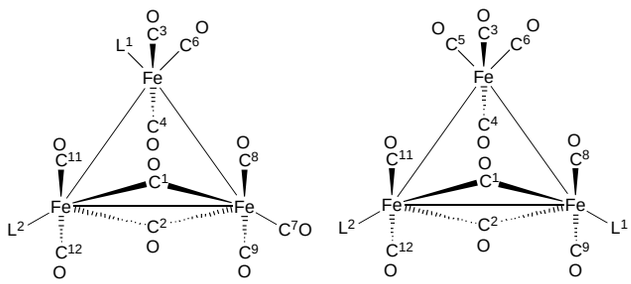

4 **5**

round exchange, see Scheme 1, but in **5** the merry-go-round is stopped, and there is a rapid axial–equatorial exchange at the unbridged six-co-ordinate iron atom. No explanation was given for this anomaly.

In 1989,[10] it was shown that for $[Fe_3(CO)_{11}\{P(OMe)_3\}]$ the intensities of the carbonyl signals are not 6:4:1 as claimed by Johnson and co-workers,[21] but are 5:5:1. These intensities could not be fitted to any of the existing published mechanisms. A new mechanism, the concerted bridge-opening bridge-closing mechanism, was proposed based on the crystal structures of $[Fe_3(CO)_{12}]$[3] and a number of its derivatives. These compounds show an asymmetric bridge for the two bridging carbonyls, and two carbonyls are approaching a semi-bridging position on a second edge. This is illustrated in Fig. 1, where the key distances are marked. It was proposed that as the carbonyl bridge on the Fe^2–Fe^3 edge of the Fe_3 triangle opens, carbonyls, C^4O and C^8O, close to bridge the Fe^1–Fe^2 edge, see Scheme 3.[10] The mechanism results in the concerted rotation of five ligands $C^1O \leftrightarrow C^{11}O \leftrightarrow C^{12}O \leftrightarrow C^2O \leftrightarrow C^7O$ about the Fe^2–Fe^3 edge, and another five ligands $C^3O \leftrightarrow C^5O \leftrightarrow C^4O \leftrightarrow C^9O \leftrightarrow C^8O$ about the Fe^1–Fe^2 edge. The cluster $[Fe_3(CO)_{10}\{P(OMe)_3\}_2]$ was re-examined.[10] It was shown to consist of two isomers, **3** and **4**, rather than **3** or **4** and **5** as proposed by Farrar and Lunniss[23] and the crystal structure of **3** was determined. In solution at −100 °C, the concerted bridge-opening bridge-closing mechanism is still very rapid for **3**, see Scheme 3, while **4**, where the mechanism has been blocked, is static. The complexes $[Fe_3(CO)_9\{P(OR)_3\}_3]$ (R = Me, Et, Pr^i or Ph) were shown to consist of two isomers in solution **6** and **7**.[10,24] In solution at −100 °C, exchange mechanisms are slow for **4** [$L^1 = L^2 = P(OMe)_3$ or $P(OPr^i)_3$] and **6** $[Fe_3(CO)_9\{P(OR)_3\}_3]$ (R = Me, Et, Pr^i or Ph) where the concerted bridge-opening bridge-closing mechanism is blocked by $P(OR)_3$ substitution, and limiting low-temperature ^{13}C NMR spectra were observed. In $[Fe_3(CO)_{11}\{P(OMe)_3\}]$ and **3** [L^1, $L^2 = CO$ and $= P(OMe)_3$ or $P(OPr^i)_3$] it was concluded that at −100 °C the concerted bridge-opening bridge-closing mechanism is rapid with $\Delta G^{\ddagger} < 25$ kJ mol^{-1}, as the mechanism is not blocked by $P(OR)_3$ substitution. The $P(OR)_3$ group has a high activation energy for going into an axial or bridging position and is an effective blocking group. Subsequently, the structure assignments for **6** and **7** were challenged by Johnson and Roberts.[25] However, recent crystal-structure determinations have shown that the original structure assignments are correct.[26]

In 1990, Johnson and Bott[11] translated this description of the concerted bridge-opening bridge-closing mechanism into the Ligand Polyhedral Model. They described a libration of the Fe_3 triangle about the C_2 axis which runs through the unbridged iron atom and bisects the bridged Fe–Fe edge of the Fe_3 triangle rather than rotation about the S_{10} axis. This mechanism produces exchange as shown in Scheme 4, which is identical to the first step of Scheme 3. The two mechanisms do differ *en route*. In the concerted bridge-opening bridge-closing mechanism, the S_{10} axis running through ligands 6 and 10 should remain co-planar with the Fe_3 triangle. In the Johnson approach, the C_2 libration moves the iron triangle so that it is no longer co-planar with the S_{10} axis. Johnson and Bott[11] did not define the angle of rotation about the C_2 axis, but as the Fe_3 triangle has to rotate 36° between **3** and **3′**, each libration must be of the order of 18°.

In 1991, Lentz and Marschall[13] published a variation on the concerted bridge-opening bridge-closing mechanism for the fluxionality of $[Fe_3(CO)_{12}]$. In 1984, Lentz and co-workers[27] had synthesised $[Fe_3(CO)_{11}(CNCF_3)]$ and shown that its structure is **8**. They carried out a variable-temperature ^{13}C NMR study and showed that at −80 °C its ^{13}C NMR spectrum agreed with the solid-state crystal structure.[27] However, at 0 °C the ^{13}C NMR spectrum showed three carbonyl signals in the intensity ratio 1:5:5. On further warming, the signal of the unique carbonyl vanishes, presumably due to a second exchange mechanism. Lentz and Marschall[13] proposed that the iron triangle rotates within the icosahedron about the pseudo S_{10} axis which runs through ligands 1 ($CNCF_3$) and 4, see Scheme 5. We pointed out that this mechanism produces the same sets of ligands exchanging as that proposed earlier using the concerted bridge-opening bridge-closing mechanism, with rotation about the pseudo C_5 axis through ligands 6 and 10.[10,28] Johnson *et al.*[29] subsequently described the mechanism in terms of the C_2 libration mechanism.

In 1990, Johnson and Bott[11] modified the Ligand Polyhedral Model from the icosahedron↔cube-octahedron↔icosahedron rearrangement to the icosahedron↔anticube-octahedron↔icosahedron rearrangement, and this fitted the merry-go-round mechanism. The ligand positions on the bridged $[Fe_3(CO)_{12}]$ approximate to those of an icosahedron, and the ligand positions on the unbridged $[Ru_3(CO)_{12}]$ and $[Os_3(CO)_{12}]$ approximate to those of an anticube-octahedron. Hence the description is identical to that of Cotton[9] for the merry-go-round given in Scheme 1, and only differs in being ligand- rather than metal-centred and in details of the movement of the metal triangle.[30] In $[Fe_3(CO)_{11}\{P(OMe)_3\}]$, $[Fe_3(CO)_{11}(CNBu^t)]$, $[Fe(CO)_{10}\{P(OMe)_3\}_2]$, $[Fe_3(CO)_{10}(CNBu^t)\{P(OMe)_3\}]$ and $[Fe_3(CO)_9\{P(OMe)_3\}_3]$, the merry-go-round mechanism has an activation energy of approximately 40 kJ mol^{-1}, while the concerted bridge-opening bridge-closing mechanism is of much lower energy.[10]

In 1992, Johnson *et al.*[31] applied the Bürgi–Dunitz approach to provide further evidence for the merry-go-round mechanism, using the Ligand Polyhedral Model. In 1993, Johnson and Roberts[25] applied the C_2 libration and the icosahedron↔anticube-octahedron↔icosahedron rearrangement to the fluxionality of $[Fe_3(CO)_{12-n}\{P(OMe)_3\}_n]$ ($n = 1$ to 3) and also reviewed the application of the Ligand Polyhedral Model to binary carbonyls.

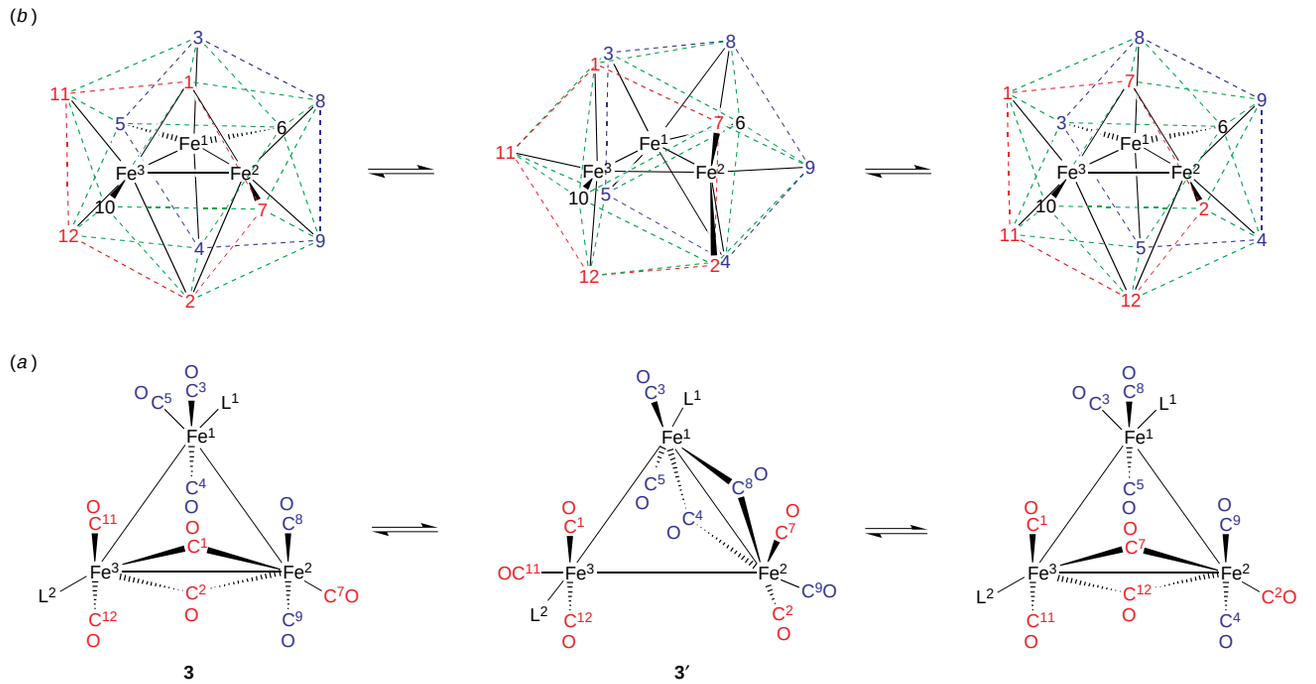

Scheme 3 The concerted-bridge-opening bridge-closing mechanism as applied to $[Fe_3(CO)_{10}L^1L^2]$, $L^1 = C^6O$, $L^2 = P(OMe)_3$. The mechanism exchanges the carbonyls $\overbrace{C^1O \leftrightarrow C^{11}O \leftrightarrow C^{12}O \leftrightarrow C^2O \leftrightarrow C^7O}$ and $\overbrace{C^3O \leftrightarrow C^5O \leftrightarrow C^4O \leftrightarrow C^9O \leftrightarrow C^8O}$. (*a*) The mechanism is represented using the Local Bonding Model. (*b*) The mechanism is represented using the Ligand Polyhedral Model, with the carbonyls represented by numbers

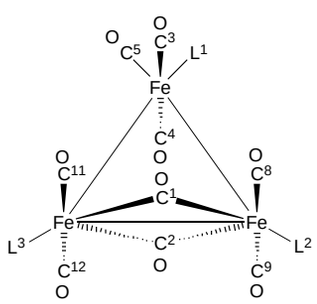

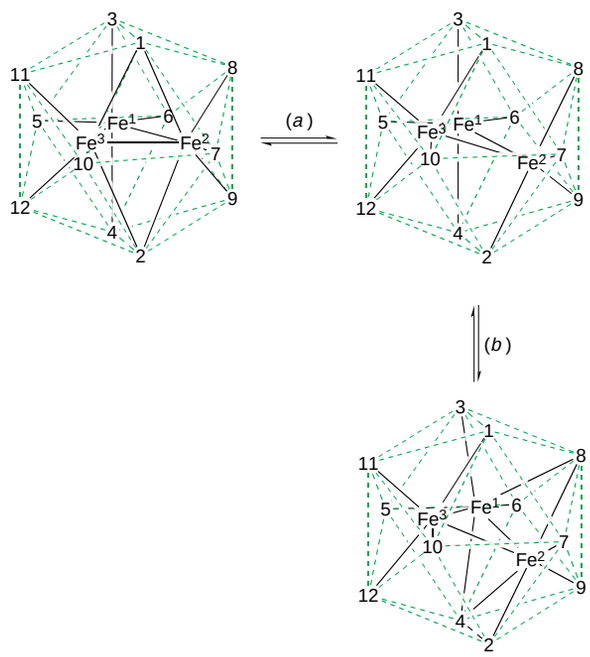

Scheme 4 The application of a libration of the Fe_3 core (*a*) about the C_2 axis which runs through the unbridged iron atom, Fe^1 and bisects the bridged Fe^2–Fe^3 edge of the Fe_3 triangle to carbonyl fluxionality in $[Fe_3(CO)_{10}L^1L^2]$ and (*b*) about the C_2 axis which runs through Fe^2 and bisects the Fe^1–Fe^3 edge of the Fe_3 triangle, to carbonyl fluxionality in $[Fe_3(CO)_{10}L^1L^2]$. The icosahedron is shown in green. Numbers are used to identify the carbonyl ligands

The variable-temperature solid-state ^{13}C magic angle spinning (MAS) NMR spectra and static spectra of $[Fe_3(CO)_{12}]$ have also been reported.[12,32] In 1986, Hanson *et al.*[12b] observed the limiting low-temperature ^{13}C NMR spectrum at −93 °C. Coalescence is observed at −55 °C and $\Delta G^{\ddagger}$ was estimated as *ca.* 42 kJ mol^{-1}. It was suggested that the fluxional mechanism consists of a 60° rotation of the Fe_3 triangle about the pseudo C_3 axis through the triangle. This suggestion followed from a proposal by Johnson in 1976.[33] Further exchange occurs above 60 °C, but no mechanism could be deduced.[32] A detailed investigation of the variable-temperature solid-state ^{13}C MAS NMR spectra of $[Fe_2Os(CO)_{12}]$ has been recently reported.[34] Detailed information on the exchange mechanism was obtained using solid-state ^{13}C exchange (EXSY) NMR spectroscopy. An exchange mechanism based on a 60° rotation coupled with a merry-go-round rearrangement was proposed. It has also been shown that $[Fe_3(CO)_{11}(PPh_3)]$ gives a solid-state ^{13}C MAS NMR spectrum at room temperature which is consistent with the molecule being static. The published crystal structure which shows two different molecules in the unit cell is not consistent with the solid-state ^{13}C and ^{31}P MAS NMR spectra which only show one type of $[Fe_3(CO)_{11}(PPh_3)]$ molecule in the solid.[35] In 1989, we suggested that, based on the ^{13}C chemical shift of the bridging carbonyl in the solid-state ^{13}C MAS NMR spectrum of $[Fe_3(CO)_{12}]$, the spectrum obtained at −93 °C was not the limiting low-temperature NMR spectrum.[10] However, in view of the subsequent work on $[Fe_3(CO)_{11}(PPh_3)]$[32] and $[Fe_2Os(CO)_{12}]$,[34] it is probable that the limiting low-temperature solid-state ^{13}C MAS NMR spectrum of $[Fe_3(CO)_{12}]$ is observed at −93 °C.

The purpose of this paper is to review and compare the descriptions of the lowest-energy fluxional processes in $[Fe_3(CO)_{12}]$ and its derivatives in both solution and solid state. The approach of Bürgi and Dunitz[19] using crystal structures to map the dynamic pathway is used.

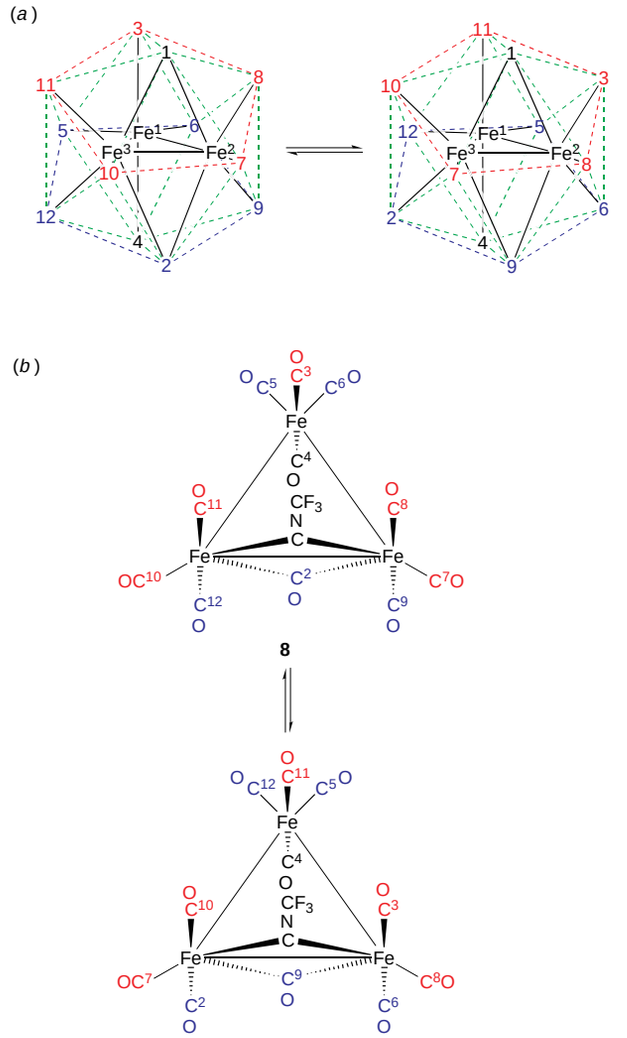

Scheme 5 The C_5 rotation about the axis through $CNCF_3$ and C^4O of $[Fe_3(CO)_{11}(CNCF_3)]$ **8** as proposed by Lentz and Marschall.[13] This mechanism produces the concerted rotation of the carbonyls $C^3O{\leftrightarrow}C^8O{\leftrightarrow}C^7O{\leftrightarrow}C^{10}O{\leftrightarrow}C^{11}O$ and $C^5O{\leftrightarrow}C^6O{\leftrightarrow}C^9O{\leftrightarrow}C^2O{\leftrightarrow}C^{12}O$. (*a*) Using the Ligand Polyhedral Model. (*b*) Using the Local Bonding Model

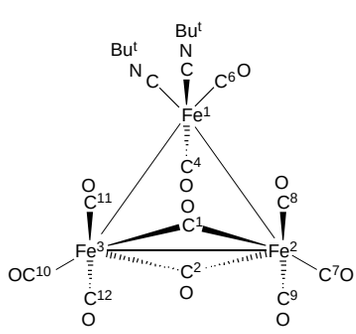

9

A Survey of the Exchange Mechanisms Observed Experimentally in $[Fe_3(CO)_{12-n}L_n]$ (n = 0–2)

In general, the lowest energy dynamic pathway in $[Fe_3(CO)_{12-n}L_n]$ is the concerted bridge-opening bridge-closing mechanism unless it is blocked by substitution, see Scheme 3. When there is no blocking ligand, this dynamic pathway is so fast in solution at −100 °C that a limiting high-temperature ^{13}C NMR spectrum is observed for the exchanging carbonyls. In all these cases $\Delta G^{\ddagger} < 25$ kJ mol^{-1}. An axial Bu^{t}NC ligand does not slow the mechanism sufficiently to produce even a broadening

Table 1 The published activation energies for the merry-go-round mechanism, see Scheme 1, in a number of $[Fe_3(CO)_{12-n}L_n]$ compounds

Compound	$\Delta G^{\ddagger}$/kJ mol^{-1}	Ref.
$[Fe_3(CO)_{11}\{P(OMe)_3\}]$	39	10
$[Fe_3(CO)_{11}(CNBu^t)]$	43	36
$[Fe_3(CO)_{11}(CNCF_3)]$	*ca.* 60	10
3 $[Fe_3(CO)_{10}L_2]$ $[L^1 = L^2 = P(OMe)_3]$	*ca.* 40	10
4 $[Fe_3(CO)_{10}L_2]$ $[L^1 = L^2 = P(OMe)_3]$	40	10
10 $[Fe_3(CO)_{10}(CNBu^t)\{P(OMe)_3\}]$	44	36
6 $[Fe_3(CO)_9L^1L^2L^3]$ $[L^1 = L^2 = L^3 = P(OMe)_3]$	41	10

of the ^{13}C NMR spectrum at 9.4 T at −100 °C, as the ligand can go into the equatorial and/or bridge position.[36] For example, in the crystal structure of $[Fe_3(CO)_{10}(CNBu^t)_2]$ **9**, one isocyanide ligand adopts an axial position and the other an equatorial one.[37] A little broadening is observed in the ^{13}C NMR spectrum of $[Fe_3(CO)_{10}\{P(OMe)_3\}(CNBu^t)]$ **10** at −100 °C and this could indicate $\Delta G^{\ddagger} = ca.$ 22 kJ mol^{-1} for the concerted bridge-opening bridge-closing mechanism. There is only one group of examples where the concerted bridge-opening bridge-closing mechanism is slowed by an isocyanide ligand to give a limiting low-temperature NMR spectrum, namely when there is a bridging $CNCF_3$ group.[13] Then the activation energy for the concerted bridge-opening bridge-closing mechanism increases to *ca.* 50 kJ mol^{-1} for $[Fe_3(CO)_{11}(CNCF_3)]$. The increase in activation energy is presumably associated with the energy associated with putting the bridging CF_3NC group into a terminal position, see below. The concerted bridge-opening bridge-closing mechanism is blocked when a phosphorus ligand is substituted at any of the exchanging sites.

The concerted bridge-opening bridge-closing mechanism is a *concerted* dynamic process, and not two independently rotating groups of five ligands. If the two sets of five ligands could rotate independently then in $[Fe_3(CO)_{10}L_2]$ **4** $[L^1 = L^2 = P(OMe)_3]$ L^1 blocks the rotation of the carbonyls C^4O, C^9O, C^8O and C^3O. The rotation of carbonyls C^1O, $C^{11}O$, $C^{12}O$, C^2O and C^7O is also blocked and a limiting low-temperature ^{13}C NMR spectrum is observed at −100 °C.[10] Similarly in **10**, the ligands Bu^{t}NC, C^5O, C^4O, C^9O and C^8O rotate around the Fe^1–Fe^2 edge and the ligands C^1O, $C^{11}O$, $C^{12}O$, C^2O and C^7O rotate around the Fe^2–Fe^3 edge. The presence of the Bu^{t}NC ligand marks a point on the two rotating pentagons of ligands. Consequently the concerted bridge-opening bridge-closing mechanism results in exchanging $C^1O{\leftrightarrow}C^{11}O$, $C^7O{\leftrightarrow}C^{12}O$, $C^5O{\leftrightarrow}C^8O$ and $C^4O{\leftrightarrow}C^9O$. There is not independent rotation of the carbonyls C^1O, $C^{11}O$, $C^{12}O$, C^2O and C^7O resulting in their averaging.

For most $[Fe_3(CO)_{12-n}L_n]$ complexes, the lowest-energy mechanism which can be monitored by ^{13}C NMR spectroscopy is the merry-go-round mechanism, see Scheme 1. In all cases, a limiting ^{13}C NMR spectrum is observed for the merry-go-round mechanism on cooling to −110 °C. On warming exchange occurs. The activation energies for the merry-go-round mechanism are collected in Table 1.

Examination of the activation energies in Table 1 shows that they fall in a narrow band, 39 to 44 kJ mol^{-1}. The only exception is $[Fe_3(CO)_{11}(CNCF_3)]$, where the $CNCF_3$ ligand is bridging and the merry-go-round involves moving it into a disfavoured axial position. It is not proven that in this case it is the merry-go-round mechanism that is occurring with $\Delta G^{\ddagger} = ca.$ 60 kJ mol^{-1}. The observed exchange could also arise from another mechanism.

The higher-temperature processes are difficult to identify. They involve exchange of groups of carbonyls which are already involved in an exchange process.

The next highest-energy dynamic process observed involves edge-bridging carbonyls. This mechanism is frequently obscured by lower-energy dynamic processes or blocked by substitution. It is observed for $[Fe_3(CO)_{10}L_2]$ **4** $[L^1 = L^2 =$

Table 2 The activation energies for a dynamic process, believed to be a trigonal twist, which is observed in $[Fe_3(CO)_{12-n}L_n]$

Compound	$\Delta G^{\ddagger}$/kJ mol^{-1}	Ref.
$[Fe_3(CO)_{11}\{P(OMe)_3\}]$	63	10
3 $[Fe_3(CO)_{10}L^1L^2]$ $[L^1 = L^2 = P(OMe)_3]$	59	10
6 $[Fe_3(CO)_9L^1L^2L^3]$ $[L^1 = L^2 = L^3 = P(OMe)_3]$	54	10

Table 3 The activation parameters for the exchange of axial carbonyls in $[Fe_3(CO)_9\{P(OR)_3\}_3]$ **7** (R = Me, Et or Pr^i) see Scheme 6

Compound	$\Delta G^{\ddagger}$/kJ mol^{-1}	Ref.
$[Fe_3(CO)_9L_3]$ $[L = P(OMe)_3]$	37.4	24
$[Fe_3(CO)_9L_3]$ $[L = P(OEt)_3]$	38.6	24
$[Fe_3(CO)_9L_3]$ $[L = P(OPr^i)_3]$	48	10

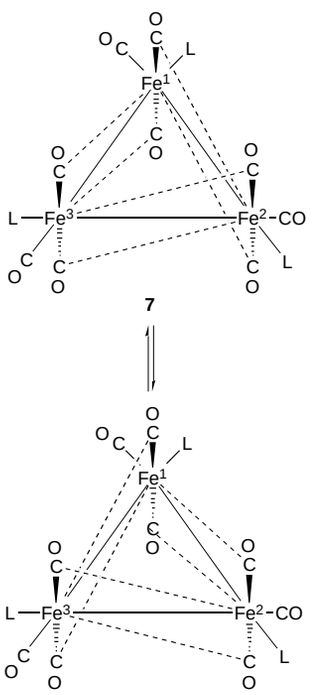

7

Scheme 6 In $[Fe_3(CO)_9\{P(OR)_3\}_3]$ **7** (R = Me, Et, Pr^i or Ph) the axial carbonyls are in semi-bridging positions. This makes the carbonyls above and below the Fe_3 triangle inequivalent. In the dynamic process they exchange roles

$P(OMe)_3]$ where it occurs with $\Delta G^{\ddagger} = 47$ kJ mol^{-1} and **4** $[L^1 = L^2 = P(OPr^i)_3]$ with $\Delta G^{\ddagger} = 48$ kJ mol^{-1}.

At higher temperatures still, another dynamic process occurs which is consistent with a local metal-centred ligand exchange, *e.g.* a trigonal twist. The published activation energies are collected in Table 2.

The group of compounds, $[Fe_3(CO)_9\{P(OR)_3\}_3]$ **7**, also undergo an exchange of the axial semi-bridging carbonyls, see Scheme 6 with an activation energy given in Table 3.

A Comparison of the C_2 Libration and Concerted-bridge-opening Bridge-closing Mechanisms of Fluxionality of $[Fe_3(CO)_{12}]$ and its Derivatives in Solution

Both the C_2 libration and concerted bridge-opening bridge-closing mechanisms produce the exchange shown in Scheme 3. They only differ in the pathway followed for the exchange. It will be shown in this discussion that the concerted bridge-opening bridge-closing mechanism is consistent with a Bürgi–Dunitz analysis of crystal-structure data.[19] Hence throughout this discussion, the mechanism will be referred to as the concerted bridge-opening bridge-closing mechanism.

In $[Fe_3(CO)_{12}]$, the molecule is very fluxional, with $\Delta G^{\ddagger} < 25$ kJ mol^{-1}, and gives a singlet in the ^{13}C NMR spectrum down to −150 °C.[2] At −100 °C, the ^{13}C NMR spectrum of $[Fe_3(CO)_{11}\{P(OMe)_3\}]$ **3** $[L^1, L^2 = CO, P(OMe)_3]$ consists of a 5:5:1 set of signals.[10] Similarly, at −100 °C, the ^{13}C NMR spectrum of **3** $[L^1 = L^2 = P(OMe)_3]$ consists of a *doublet*, showing that although all ten carbonyls are averaged by exchange they consist of two sets of five, each set being close to only one $P(OMe)_3$ ligand.[10] This is consistent with Scheme 3, where the set of carbonyls $\overline{C^1O \leftrightarrow C^{11}O \leftrightarrow C^{12}O \leftrightarrow C^2O \leftrightarrow C^7O}$ remains associated with the Fe^2–Fe^3 edge of the Fe_3 triangle and L^2 and the set of carbonyls $\overline{C^3O \leftrightarrow C^5O \leftrightarrow C^4O \leftrightarrow C^9O \leftrightarrow C^8O}$ remains associated with the Fe^1–Fe^2 edge of the Fe_3 triangle and L^1. When the phosphorus ligand is in any other site than that of L^1 or L^2 in **3**, the concerted bridge-opening bridge-closing mechanism is blocked and the limiting low-temperature NMR spectrum is obtained at −100 °C. The blocking by phosphorus ligands arises because the ligands appear to have a strong preference for equatorial sites. This is what is found for $[Fe_3(CO)_{10}\{P(OR)_3\}_2]$ **4**[10] and $[Fe_3(CO)_9\{P(OR)_3\}_3]$ **6**.[10,24,26]

In the case of isocyanide derivatives, the isocyanide ligand does not block the concerted bridge-opening bridge-closing mechanism. It is known that isocyanide ligands can go into the equatorial position,[37] and can transfer between the metal atoms by bridging.[38–40] For $[Fe_3(CO)_{11}(CNBu^t)]$, the crystal structure shows the isocyanide ligand to be in the axial position on the unbridged iron atom, **11**.[41] The ^{31}C NMR spectrum of $[Fe_3(CO)_{11}(CNBu^t)]$ at −100 °C consists of three signals at δ 242.2, 215.6 and 207.6, with intensities 1:5:5.[36] There are two pathways for carbonyl exchange by the concerted bridge-opening bridge-closing mechanism in $[Fe_3(CO)_{11}(CNBu^t)]$. Scheme 7 shows a mechanism involving the isocyanide ligand moving into an equatorial position. Once it has become equatorial, the sets of carbonyls become equivalent by the operation of the concerted bridge-opening bridge-closing mechanism about the Fe^1–Fe^3 and Fe^2–Fe^3 edges. Scheme 8 shows the alternative mechanism where the isocyanide ligand bridges.

The case of $[Fe_3(CO)_{11}(CNCF_3)]$ requires separate discussion and is considered in detail later.[13] There have been no reports of the concerted bridge-opening bridge-closing mechanism occurring in derivatives of $[Ru_3(CO)_{12}]$ or $[Os_3(CO)_{12}]$. Consequently, the discussion of this mechanism will be restricted to $[Fe_3(CO)_{12}]$ and its derivatives.

At first sight, the concerted bridge-opening bridge-closing mechanism may appear to be rather perverse.‡ As normally drawn, C^1O and C^2O appear to be a long way from C^7O. However, examination of the crystal structures of $[Fe_3(CO)_{12}]$ and its derivatives show that carbonyls C^7O, C^1O, C^2O, $C^{11}O$ and $C^{12}O$ are approximately co-planar as are carbonyls C^8O, C^9O, C^3O, C^4O and C^5O, with the carbons deviating only 0.05 and 0.07 Å from the mean plane through each set, see Fig. 2(*a*) and 2(*b*). The two planes are not quite parallel, being inclined at an angle of 8° in $[Fe_3(CO)_{12}]$ at 100 K.[4] As Wei and Dahl, and Corradini and Paiaro have independently concluded, the carbonyl ligands form an approximate icosahedron.[2,20] Using this representation, carbonyls C^6O and $C^{10}O$ form opposite apices of the icosahedron. When the Fe_3 triangle is placed in the plane of the paper, see Fig. 2(*a*), or when the ligands C^6O and $C^{10}O$ and Fe^2 are put in the plane of the paper, see Fig. 2(*b*), it can be seen that carbonyls C^7O, C^1O, C^2O, $C^{11}O$ and $C^{12}O$, and C^8O, C^9O, C^3O, C^4O and C^5O form two nearly parallel planes, with an angle of 8° between them. Viewed down the C^6O–$C^{10}O$ axis, the two sets of carbonyls, C^7O, C^1O, C^2O, $C^{11}O$ and $C^{12}O$, and

‡ The reader could be assisted in understanding the discussion by downloading the structures of $[Fe_3(CO)_{12}]$, GAFMEFO2, and $[Fe_3(CO)_{10}\{1,2\text{-}(Me_2As)_2C_6H_4\}]$, MASCFE, from the Cambridge Crystallographic DataBase, and examining them using a viewing program such as Chem 3D.

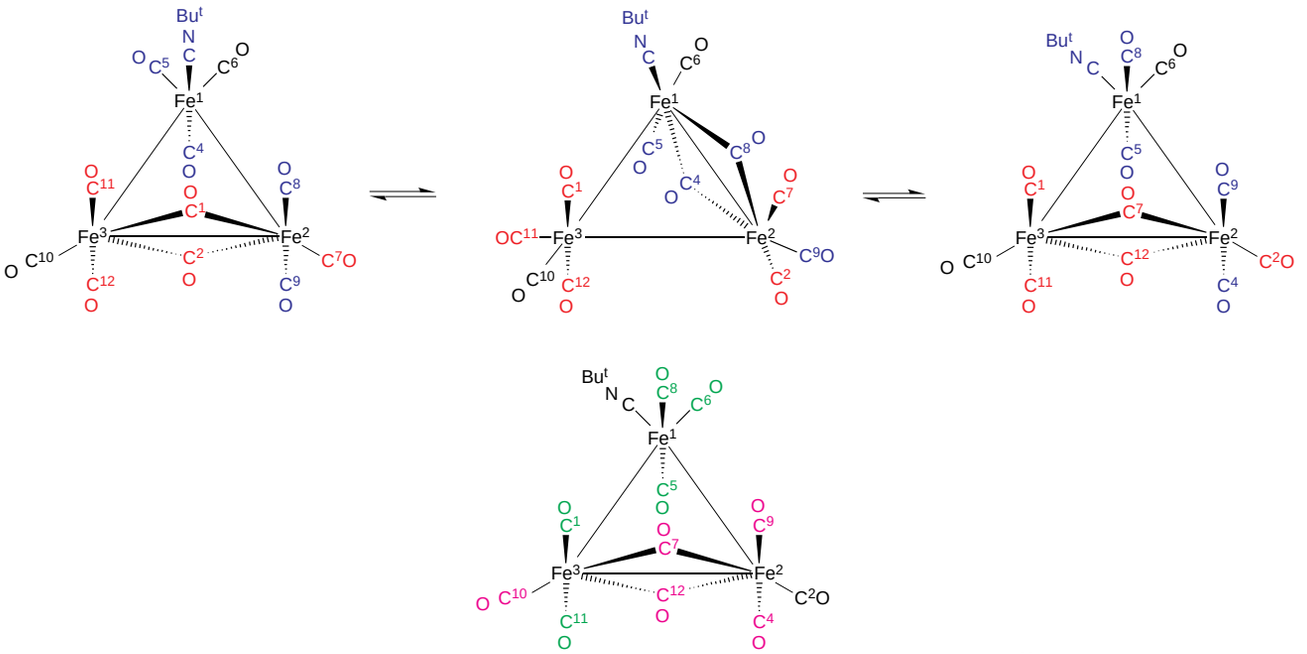

Scheme 7 The application of the concerted-bridge-opening bridge-closing mechanism to $[Fe_3(CO)_{11}(CNBu^t)]$ **11**.[36] Firstly there is rotation of the carbonyls and the isocyanide around the Fe^1–Fe^2 and Fe^3–Fe^2 edges of the Fe_3 triangle to move the isocyanide into the equatorial position. This then allows concerted rotation of the carbonyls $C^1O \leftrightarrow C^8O \leftrightarrow C^6O \leftrightarrow C^5O \leftrightarrow C^{11}O$ and $C^{10}O \leftrightarrow C^7O \leftrightarrow C^9O \leftrightarrow C^4O \leftrightarrow C^{12}O$ around the Fe^3–Fe^1 and Fe^3–Fe^2 edges of the Fe_3 triangle

C^8O, C^9O, C^3O, C^4O and C^5O, form two flattened pentagons, see Fig. 2(*c*). There is an approximate S_{10} axis running through C^6O and $C^{10}O$. The concerted bridge-opening bridge-closing mechanism is then described as a 36° rotation of the icosahedron or the Fe_3 triangle about the axis defined by C^6O and $C^{10}O$. The axis through C^6O and $C^{10}O$ is not completely parallel to the Fe^1–Fe^3 edge. This is because the bridged edge, Fe^2–Fe^3 is shorter than the unbridged edge, Fe^1–Fe^2. As the S_{10} rotation proceeds these two edges will exchange roles and alternatively lengthen and shorten.

Strong evidence for the rotation of the icosahedron of carbonyls about the C^6O–$C^{10}O$ vector comes from the crystal structure of $[Fe_3(CO)_{10}\{1,2\text{-}(Me_2As)_2C_6H_4\}]$ **12**[42] which has the structure which is approximately halfway between the two ligand arrangements **3** and **3′**. This is easily seen by comparing Figs. 2(*c*) and 3, which are projections along the vector defined by the carbons atoms of C^6O and $C^{10}O$.

In comparison with the idealised structure with ligands 5 and 7 co-planar with the iron triangle, in $[Fe_3(CO)_{10}\{1,2\text{-}(Me_2As)_2C_6H_4\}]$ **12** the ligands have rotated around the Fe_3 triangle by 18.45° on average. The driving force for this rotation is both arsenic atoms trying to become co-planar with the iron triangle as is normally found. The rotation of 18.45° is very close to the 'ideal' 18° predicted for the mid-point at the S_{10} rotation. It is at this point the concerted bridge-opening bridge-closing mechanism and the C_2 libration mechanism can be most effectively compared. According to the concerted bridge-opening bridge-closing mechanism, the S_{10} axis, as defined by the line joining ligands 6 and 10 should remain co-planar with the Fe_3 plane. With the C_2 libration mechanism a substantial deviation is to be expected. Johnson has not defined the degree of rotation associated with the C_2 rotation. However, the two C_2 librations must produce an overall rotation of the Fe_3 triangle of 36° as defined in Scheme 3. It can therefore be concluded that each C_2 libration produced a rotation of approximately 18°. For $[Fe_3(CO)_{10}\{1,2\text{-}(Me_2As)_2C_6H_4\}]$ **12** the angle is 2.6°. The corresponding angle for $[Fe_3(CO)_{12}]$ at 100 K is 2.2° on average. It can therefore be concluded that these data provide no evidence for the C_2 libration mechanism.

Examination of the Fe–Fe bond lengths of $[Fe_3(CO)_{10}\{1,2\text{-}(Me_2As)_2C_6H_4\}]$ shows that they are consistent with this molecule being approximately halfway between **3** and **3′** in Scheme 3. The Fe^1–Fe^3 and Fe^2–Fe^3 bond lengths are approximately equal at 2.602(1) and 2.597(1) Å,[4] which can be compared with the bridging and terminal bond lengths found in $[Fe_3(CO)_{12}]$ at 100 K of 2.540(1) and 2.675(1)–2.682(1) Å.[4] The Fe^1–Fe^2 bond is nearly on the rotation axis and is not substantially affected having a bond length of 2.662(1) Å in $[Fe_3(CO)_{10}\{1,2\text{-}(Me_2As)_2C_6H_4\}]$.[42]

The Cambridge Crystallographic Data Base[43] has been searched for all relevant compounds, and the positions of the carbonyls has been examined. Further evidence for the rotation of the carbonyls around the Fe_3 triangle within the icosahedron of carbonyls about the pseudo S_{10} axis comes from examining the positions of the carbonyls about the iron triangle. This is shown in Fig. 4, where the position of the carbon, oxygen and iron atoms derived from the crystal structures of $[Fe_3(CO)_{12}]$,[3] $[Fe_3(CO)_{12}]$ at 100 K,[4] $[Fe_3(CO)_{11}(CNBu^t)]$,[41] $[Fe_3(CO)_{11}(\mu\text{-}CNCF_3)]$,[27] $[Fe_3(CO)_{11}(NCC_6H_4Me\text{-}2)]$,[44] $[Fe_3(CO)_{11}(PPh_3)]$,[35] $[(OC)_{11}Fe_3Ph_2P(CH_2)_6(PPh_2)Fe_3(CO)_{11}]$,[45] $[Fe_3(CO)_{10}(CNBu^t)_2]$,[37] $[Fe_3(CO)_{10}(CNBu^t)\{P(OMe)_3\}]$,[36] $[Fe_3(CO)_{10}(\mu\text{-}CNCF_3)(PMe_3)]$,[13] $[Fe_3(CO)_{10}(\mu\text{-}CNCF_3)\{P(OMe)_3\}]$ (both isomers),[13] $[Fe_3(CO)_{10}\{P(OMe)_3\}_2]$,[10] $[Fe_3(CO)_{10}\{1,2\text{-}(Me_2As)_2C_6H_4\}]$,[42] $[Fe_3(CO)_{10}\{Fe(\eta^5\text{-}C_5H_4PPh_2)_2\}]$,[46] $[Fe_3(CO)_{10}\{Me_2AsC{=}C(AsMe_2)CF_2CF_2\}]$,[47] $[Fe_3(CO)_9(PMe_2Ph)_3]$[48] and $[Fe_3(CO)_9\{P(OMe)_3\}_3]$[26] are given. Phosphorus and arsenic ligands are always placed if possible in positions 6 and/or 10.

Fig. 4(*a*) shows the iron atoms and carbonyl ligand positions plotted for all the compounds in Table 4. The molecules have been aligned so that the S_{10} axis through ligands 6 and 10 is orthogonal to the paper and the Fe^2 atoms are coincident. Examination of Fig. 4(*a*) shows a well defined circuit for the groups of five carbonyls to move around the iron triangle. These consist of two groups of five carbonyls which lie in separate planes. This is shown in Fig. 4(*b*), where the molecules have been rotated 90° around the axis at right angles to the S_{10} axis and Fe^2. The two planes defined by the carbonyls C^1O, C^2O, C^7O, $C^{11}O$ and $C^{12}O$ and C^3O, C^4O, C^5O, C^8O and C^9O are actually slightly inclined to each other, with an angle of approximately 8°. It can be seen that both these planes are approximately at right angles to the iron triangle. In Fig. 4(*c*) only the carbonyl groups C^1O, C^2O, C^7O, $C^{11}O$ and $C^{12}O$, and

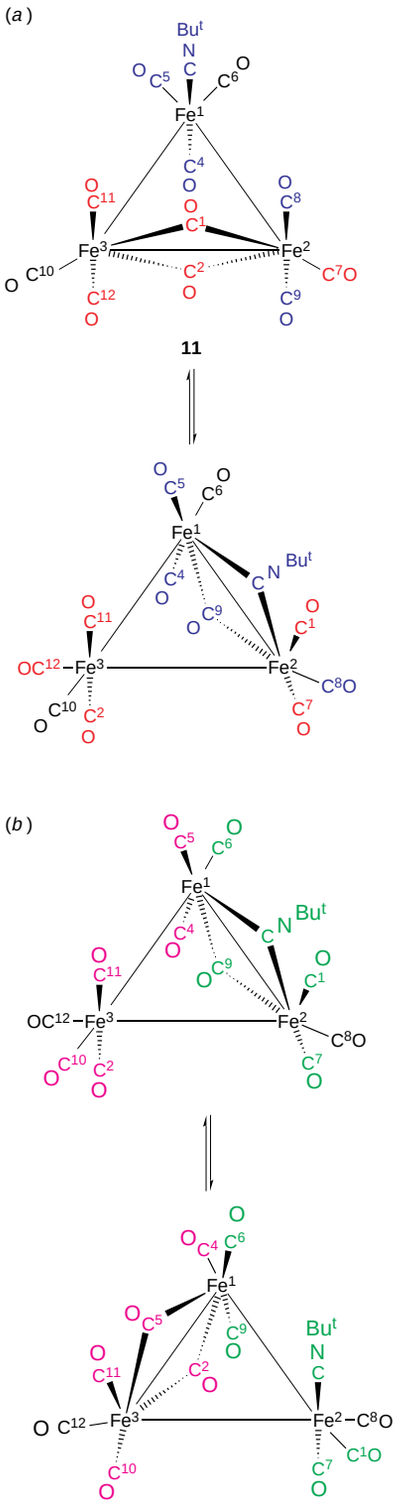

Scheme 8 An alternative application of the concerted-bridge-opening bridge-closing mechanism to $[Fe_3(CO)_{11}(CNBu^t)]$ **11**, involving the $CNBu^t$ ligand going bridging.[36] (*a*) First there is exchange along the Fe^2–Fe^1 and Fe^2–Fe^3 edges of the Fe_3 triangle to put the isocyanide ligand bridging. (*b*) There is then exchange along the Fe^1–Fe^2 and Fe^1–Fe^3 edges of the Fe_3 triangle. The overall result is movement of the isocyanide ligand from Fe^1 to Fe^2. The exchange sequence is $C^1O \leftrightarrow C^6O \leftrightarrow C^{11}O \leftrightarrow C^8O \leftrightarrow C^5O$ and $C^4O \leftrightarrow C^{10}O \leftrightarrow C^9O \leftrightarrow C^{12}O \leftrightarrow C^7O$

the iron atoms Fe^2 and Fe^3 are shown. Similarly, in Fig. 4(*d*) only the carbonyl groups C^3O, C^4O, C^5O, C^8O and C^9O, and the iron atoms Fe^1 and Fe^2 are shown. Fig. 4(*c*) shows the pathway followed by carbon atoms C^1O, C^2O, C^7O, $C^{11}O$ and $C^{12}O$ in the crystal structures, while Fig. 4(*d*) shows the pathway followed by carbon atoms C^3O, C^4O, C^5O, C^8O and C^9O. The gaps in the

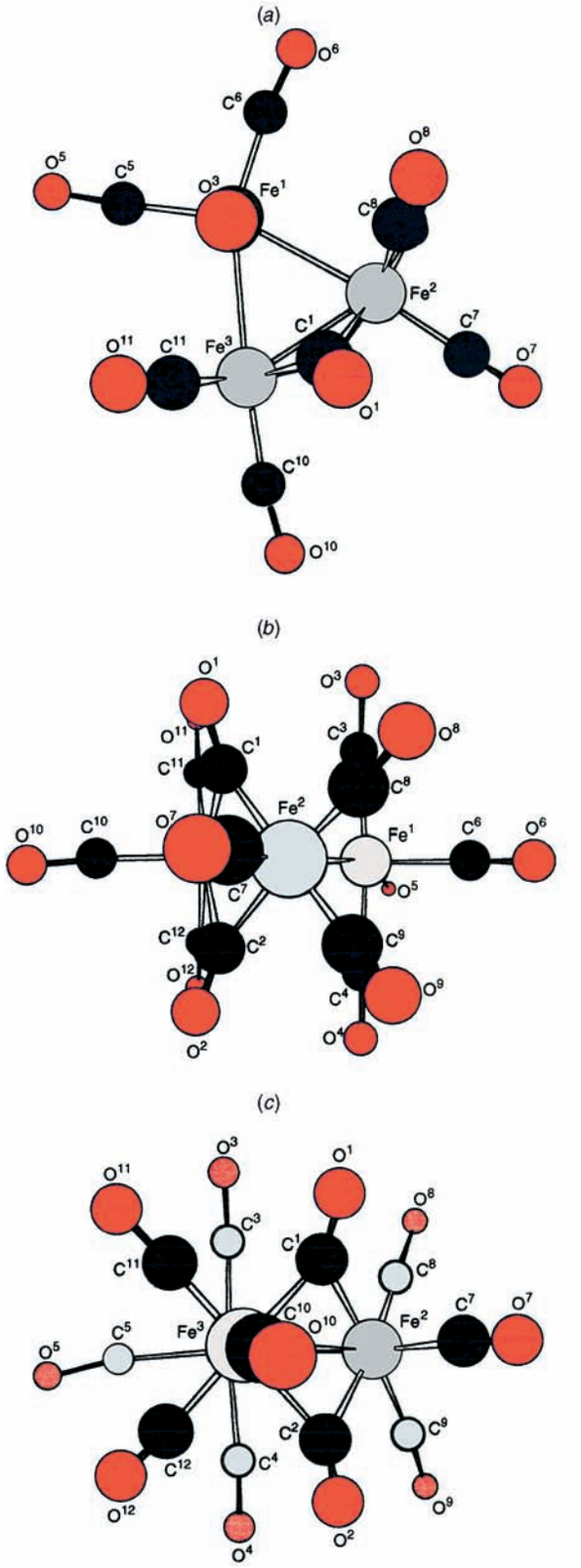

Fig. 2 Three projections taken from the crystal structure of $[Fe_3(CO)_{12}]$ at 100 K.[4] The iron atoms are shown in grey, the carbon atoms in black, and the oxygen atoms in red. The numbers 1–12 refer to the atom numbering as in compound **1**. (*a*) A projection with the carbonyl carbon atoms 6 and 10 and Fe^2 in the plane of the paper. (*b*) A projection with the carbonyl carbon atoms 6 and 10 along the *x* axis (horizontal), and these carbon atoms and Fe^2 lying in the *xz* plane (the *z* axis is orthogonal to the plane of the paper). Projections (*a*) and (*b*) are chosen to demonstrate the approximate planarity of the two groups of carbonyls 1, 12, 11, 2, 7 and 3, 5, 4, 9, 8. (*c*) A projection looking along the vector joining carbonyl carbons 6 and 10. This projection demonstrates how the two groups of carbonyls 1, 12, 11, 2, 7 and 3, 5, 4, 9, 8 form approximate pentagons. Paler colouring is used for the atoms associated with the five ligands forming the back pentagon

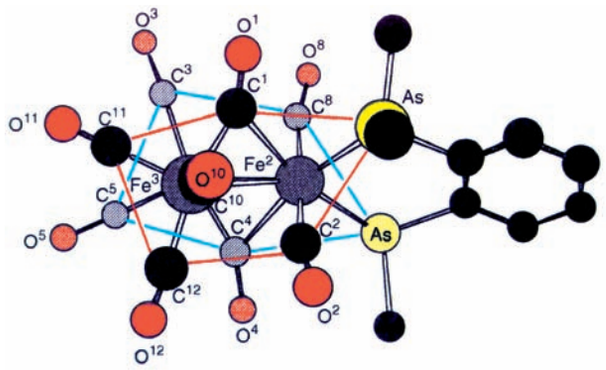

Fig. 3 A projection taken from the crystal structure of $[Fe_3(CO)_{10}\{1,2\text{-}(Me_2As)_2C_6H_4\}]$.[43] The iron atoms are shown in grey, the carbon atoms in black and the oxygen atoms in red. The numbers 1–12 refer to the atom numbering as in compound **1** with carbonyls C^7O and C^8O replaced by $1,2\text{-}(Me_2As)_2C_6H_4$. The projection looks along the vector joining carbonyl carbons 6 and 10. Carbonyl carbon and oxygen atoms 6, iron atom 1, and one of the methyl groups attached to arsenic atoms are omitted for clarity. The group of four carbonyls and one arsenic at the front of the projection are joined by a red line, while the group of four carbonyls and one arsenic at the back of the projection are joined by a blue line. Paler colouring is used for the atoms associated with the five ligands forming the back pentagon

rotation pathways in Fig. 4(*c*) and 4(*d*) arise because C^1O and C^2O are chosen to be the most bridging carbonyls. The result is that each Fig. contains blocks of carbonyl positions covering an arc of 36° followed by a gap of 36°. Local deformations due to ligands help to produce a spread of carbonyl ligands around the S_{10} rotation axis. Bürgi and Dunitz[19] have shown that such plots are valuable in mapping out the pathway of a dynamic process, and Crabtree and Lavin[18] and subsequently Johnson *et al.*[31] have applied the same approach to defining the pathway followed by the carbon atoms during the merry-go-round mechanism.

Examination of Fig. 4(*b*) provides little support for Johnson's theory of a C_2 libration. This would take the plane of the Fe_3 triangle out of the plane of the vector between ligands 6 and 10. Table 4 gives the angle between the vector through the ligands 6 and 10 and the Fe_3 plane and the degree of rotation about the pseudo S_{10} axis through ligands 6 and 10 derived from crystal structures. There is no correlation, showing that the crystal structural evidence provides no support for Johnson's C_2 libration.

There is one relevant compound not included in Table 4, $[Fe_3(CO)_9\{P(OPr^i)_3\}_3]$ **7**.[26] This compound adopts a structure similar to that found for $[Ru_3(CO)_9\{P(OEt)_3\}_3]$, based on an anticube-octahedron.[49] Due to the stereochemistry of the $P(OPr^i)_3$ ligands, the compound cannot adopt the usual geo-

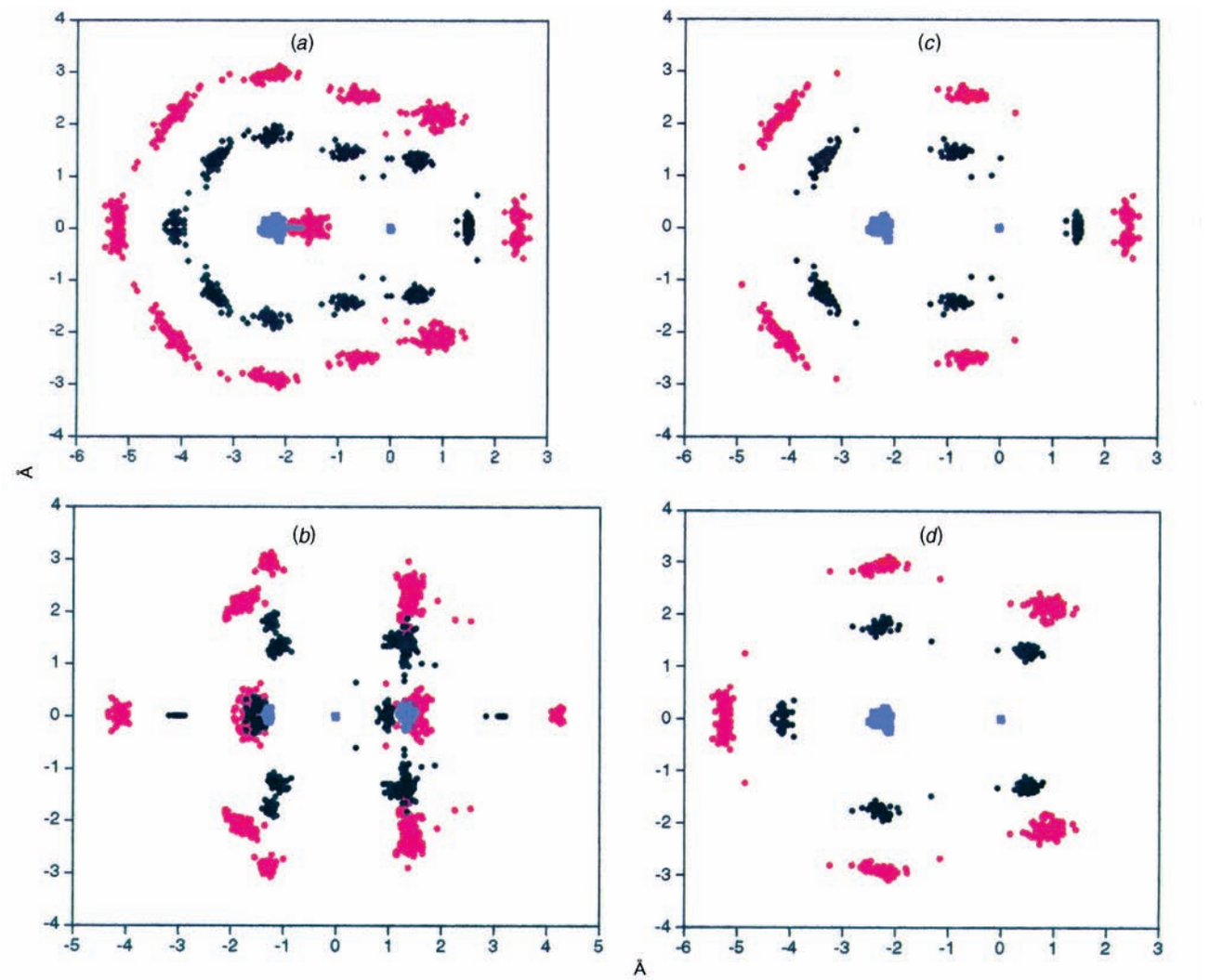

Fig. 4 Plots of the carbon and iron positions derived from crystal structures of $[Fe_3(CO)_{12-n}L_n]$ as defined in the text. Only iron atoms and the carbonyl and isocyanide (carbon) groups are included. The carbon atoms are shown in black, oxygen atoms in red and the iron atoms in blue. (*a*) All the atoms are shown, viewed along the Fe^1–Fe^3 bond with Fe^2 in the *x* direction (horizontal). (*b*) As for (*a*) but rotated 90° about the axis orthogonal to L^6, L^{10} and Fe^2. (*c*) As for (*a*) showing only carbon atoms, C^1, C^2, C^7, C^{11} and C^{12} and the iron atoms. (*d*) As for (*a*) showing only carbon atoms, C^3, C^4, C^5, C^8 and C^9 and the iron atoms. In Fig. 4(*a*), 4(*c*) and 4(*d*) the number of points have been doubled by reflecting the carbon and oxygen atoms across the L^6, L^{10} and Fe^2 plane

Table 4 Crystallographic data for $[Fe_3(CO)_{12}]$ and its derivatives

Compound	Angle between Fe_3 plane and 6–10 vector/°	Rotation about pseudo S_{10} axis/°	Ref.	Cambridge Crystallographic Database code
$[Fe_3(CO)_{12}]$	2.37	2.86	3	GAFMEF01
	3.03	2.76		
$[Fe_3(CO)_{12}]$ at 100 K	1.59	1.82	4	GAFMEF02
	2.87	1.45		
$[Fe_3(CO)_{11}(CNBu^t)]$	3.48	0.45	41	CAMZIZ
	1.28	1.89		
$[Fe_3(CO)_{11}(CNCF_3)]$ molecule 1	0.10	0.57	27	COHHUC
	0.10	1.26		
Molecule 2	0.71	0.53	27	COHHUC
	1.89	0.39		
$[Fe_3(CO)_{11}(NCC_6H_4Me\text{-}2)]$ [a]	1.71	3.30	44	JAFPAH
	2.50	3.68		
$[Fe_3(CO)_{11}(PPh_3)]$ molecule 1	1.52	2.20	35	PHOFEC10
Molecule 2	1.30	4.17	35	PHOFEC10
$[(OC)_{11}Fe_3Ph_2P(CH_2)_6(PPh_2)Fe_3(CO)_{11}]$	4.83	6.32	45	KIKLUL
$[Fe_3(CO)_{10}(CNBu^t)_2]$	0.84	1.93	37	SEYGIM
$[Fe_3(CO)_{11}(CNBu^t)\{P(OMe)_3\}]$	1.06	0.33	36	
$[Fe_3(CO)_{11}(CNBu^t)\{P(OMe)_3\}]$	2.17	0.66	36	
$[Fe_3(CO)_{10}(\mu\text{-}CNCF_3)(PMe_3)]$	1.85	1.99	13	VITHUB
$[Fe_3(CO)_{10}(CNCF_3)\{P(OMe)_3\}]$ isomer I	1.34	0.60	13	VITJAJ
Isomer II	0.82	2.39	13	VITJAK
$[Fe_3(CO)_{10}\{P(OMe)_3\}_2]$	0.53	0.45	10 [a]	JATNUN
$[Fe_3(CO)_{10}\{1,2\text{-}(Me_2As)_2C_6H_4\}]$	2.62	18.45	42 [b]	MASCFE
$[Fe_3(CO)_{10}\{Me_2AsC{=}C(AsMe_2)CF_2CF_2\}]$, molecule 1	0.32	1.11	47 [c]	FEBFEC
	0.14	1.27		
Molecule 2	5.54	0.59	47 [c]	FCBFEC
	2.93	5.23		
$[Fe_3(CO)_{10}\{Fe(\eta^5\text{-}C_5H_4PPh_2)_2\}]$	3.13	4.20	46 [d]	VUPJAR
	2.53	4.29		
$[Fe_3(CO)_9(PMe_2Ph)_3]$	0.28	1.48	48	CMPPFE10
$[Fe_3(CO)_9\{P(OMe)_3\}_3]$	2.08	2.10	26	

[a] Only the major conformer is included, on account of the large errors in the coordinates of the minor isomer. [b] Fe^3 was taken as being the iron atom substituted with the diarsenic ligand. [c] This structure provided four entries due to the two different molecules in the unit cell and the choice of two arsenic-substituted iron atoms for Fe^2. [d] This structure provided two entries due to the choice of two phosphorus-substituted iron atoms for Fe^2.

metry with one Fe–Fe edge bridged by two carbonyls, with the S_{10} rotation being blocked. Instead, the axial carbonyls lean towards semi-bridging positions. The result is a rotation of an average of 24° of the P–Fe–C plane with respect to the Fe_3 triangle. This puts an average angle of 10.5° between the Fe_3 plane and the 6–10 vector. This could be viewed as the intermediate/transition state required for the C_2 libration mechanism. However, the activation energy for the C_2 libration of the $Fe(CO)_3\{P(OPr^i)_3\}$ moiety is 48 kJ mol^{-1},[10] see Table 3, which is much higher than the <25 kJ mol^{-1} found for the lowest-energy dynamic pathway, and this structure cannot lie on the lowest-energy dynamic pathway.

Further support for the rotation about the S_{10} axis comes from the disorder observed in the crystal structure of $[Fe_3(CO)_{10}\{P(OMe)_3\}_2]$.[10] There are two positions for the Fe_3 triangles with occupancies of 0.887 and 0.113.§ The two triangles are related to each other by a rotation of 147° about the axis through the P–P axis, see Fig. 5. An idealised rotation of $^4S_{10}$ or $^2C_5$ about this axis would produce an angle of 144°.

Johnson and co-workers[4] have argued that the thermal ellipsoids derived from the crystal structure of $[Fe_3(CO)_{12}]$ provide evidence for the C_2 libration. The thermal ellipsoids clearly show a greater motion for Fe^2 and Fe^3 than for Fe^1. This is consistent with the C_2 libration, but also with an oscillation about the pseudo S_{10} axis. Due to the absence of ligands other than carbonyl in $[Fe_3(CO)_{12}]$, there are no constraints of the pseudo S_{10} axis through ligands 6 and 10, which mainly affects Fe^2 but the rotation can also be through ligands 5 and 7, which mainly affects Fe^3. The result is that Fe^2 and Fe^3 will have substantial thermal ellipsoids orthogonal to the Fe_3 plane as is observed.

§ In order to check if this is an artefact, fresh crystals have been grown, and occupancies of 0.90:0.10 found.

The Fluxionality of $[Fe_3(CO)_{11}(CNCF_3)]$

Lentz and co-workers[27] have found that the ^{13}C NMR spectrum of $[Fe_3(CO)_{11}(CNCF_3)]$ **8** at −80 °C agrees with the crystal structure. On warming exchange occurs. In 1991, Lentz and Marschall[13] suggested a mechanism involving rotation of the Fe_3 triangle about the pseudo S_{10} axis going through positions 1 and 4, see Scheme 5. This mechanism is suitable for $[Fe_3(CO)_{11}(CNCF_3)]$ but is blocked in many of the other compounds studied by phosphorus ligand substitution.

The fluxionality of $[Fe_3(CO)_{11}(CNCF_3)]$ has an activation energy of *ca.* 50 kJ mol^{-1} (estimated from the ^{13}C NMR spectra in Fig. 8 of ref. 16). This is considerably higher than the <25 kJ mol^{-1} found for $[Fe_3(CO)_{12}]$.[15] It is difficult to see any reason for the mechanism given in Scheme 5 to have a substantially higher activation energy in $[Fe_3(CO)_{11}(CNCF_3)]$ than in $[Fe_3(CO)_{12}]$ as the same carbonyl ligands are moving and the $CNCF_3$ group is fixed. It is therefore concluded that this mechanism does not give rise to the very low energy carbonyl exchange mechanism found in $[Fe_3(CO)_{12-n}\{P(OMe)_3\}_n]$ ($n = 0$ to 2).[10]

There is a substantial problem associated with the C_5 rotation about the axis through the ligands in the 1 and 4 positions. Using the Ligand Polyhedral Model, such a mechanism looks feasible, but when the mechanism is transposed to a model using the Localised Bonding Model, the mechanism is unprecedented, see Scheme 9. The intermediate/transition state, **13**, represents a bonding arrangement which is completely unknown. This does not mean that it is impossible, but the fluxionality of $[Fe_3(CO)_{11}(CNCF_3)]$ can be fully explained using

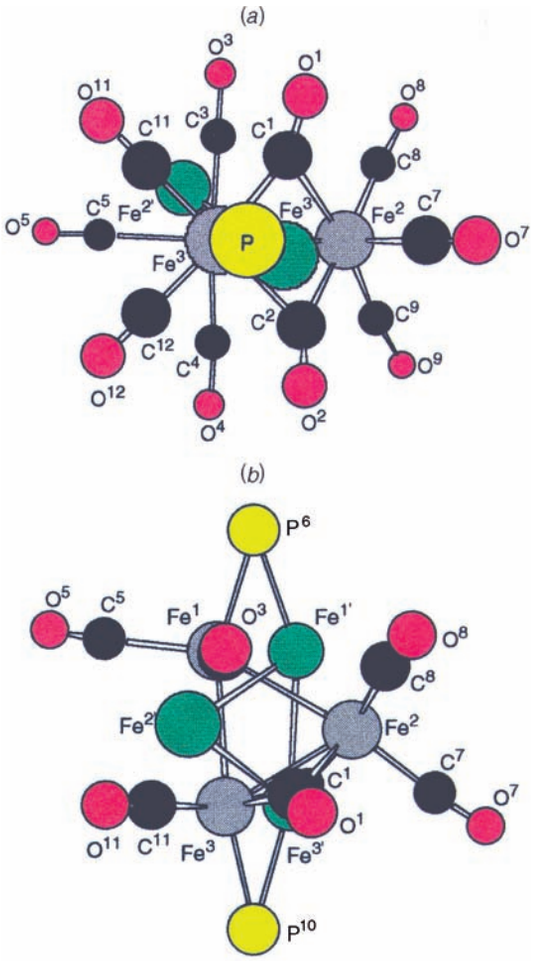

Fig. 5 A projection of the crystal structure of $[Fe_3(CO)_{10}\{P(OMe)_3\}_2]$ (*a*) so that the P–P vector lies at right angles to the plane of the paper and the Fe_3 triangle due to the iron atoms in the major sites lies approximately horizontal and (*b*) so that the two phosphorus atoms and Fe^2 lie in the plane of the paper.[10] The iron atoms are shown in grey, the carbon atoms in black and the oxygen atoms in red. The numbers 1–12 refer to the atom numbering as in compound **3**, with P^6 replacing L^1 and P^{10} replacing L^2. The methoxy groups of the phosphite are omitted. The iron atoms of the second minor form are also shown, coloured green. In the minor form, the Fe_3 triangle has rotated by 147° about the S_{10} axis which runs through the P–P vector

the concerted bridge-opening bridge-closing mechanism discussed above. An exchange mechanism has already been published involving a seven step exchange pathway.[28] This mechanism involved restricting the concerted bridge-opening bridge-closing mechanism to two edges of the Fe_3 triangle. However, if all three edges are used, then a two-step mechanism is possible, see Scheme 10. The increase in the activation energy for the concerted bridge-opening bridge-closing mechanism arises from the difficulty in moving the $CNCF_3$ ligand from the bridging to the terminal position. This does not mean that **13** is the transition state. It has been shown that for $[Ir_4(CO)_{11}(PH_2Ph)]$ and $[Ir_4(CO)_{11}(PHPh_2)]$ the transition state lies between the bridge and terminal forms.[50]

In $[Fe_3(CO)_{10}(CNCF_3)\{P(OMe)_3\}]$ **14** the mechanism in Scheme 10 is blocked by $P(OMe)_3$ substitution. The $P(OMe)_3$ ligand is an equatorial position on the bridges edge, the positions occupied by C^7O or $C^{10}O$. The dynamic process in Scheme 10 would put the $P(OMe)_3$ ligand into a high-energy axial position. The original four-step mechanism is still allowed,[28] where a $P(OMe)_3$ ligand in the position of $C^{10}O$ would remain equatorial. The activation energy increases from 42 kJ mol^{-1} in $[Fe_3(CO)_{11}(CNCF_3)]$ **8** to 55 kJ mol^{-1} in $[Fe_3(CO)_{11}(CNCF_3)\{P(OMe)_3\}]$ **14**.[13] This could be due to the lower stability of an intermediate with the equatorial $CNCF_3$ ligand in the original mechanism.[28]

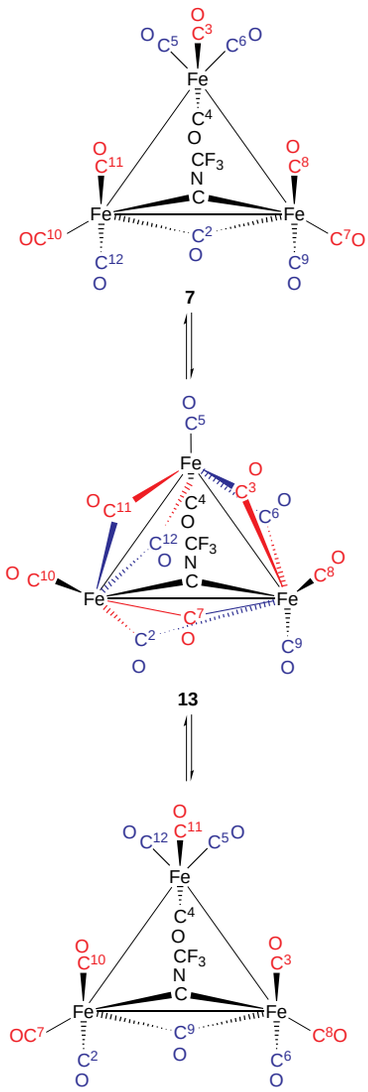

Scheme 9 The C_5 rotation about the axis through $CNCF_3$ and C^4O of $[Fe_3(CO)_{11}(CNCF_3)]$ **7** as proposed by Lentz and Marschall.[13] Compound **13** represents the halfway stage of the exchange mechanism shown using the Local Bonding Model

Fluxionality of $[Fe_3(CO)_{12}]$ and $[Fe_2Os(CO)_{12}]$ in the Solid State

In the solid state, dynamic processes which occur readily in solution may be considerably slower due to the difficulty of movement in a close-packed solid. For example, cyclooctatetraene rotation in $[Fe(CO)_3(\eta^4\text{-}C_8H_8)]$ occurs with $\Delta G^{\ddagger} = 28.5$ kJ mol^{-1} in solution,[51] and 38 ± 1 kJ mol^{-1} in the solid state.[52] The fluxionality of organometallic compounds in the solid state has recently been reviewed.[53]

It can therefore be anticipated that any fluxional process found in $[Fe_3(CO)_{12}]$ and its derivatives in solution will have an equal or higher activation energy in the solid state. An activation energy of 42 kJ mol^{-1} has been reported for the fluxionality of $[Fe_3(CO)_{12}]$ in the solid state.[12] On the basis of measurements in solution, only two mechanisms are possible, the concerted bridge-opening bridge-closing and the merry-go-round mechanisms.

The fluxionality of $[Fe_3(CO)_{12}]$[12,34] and $[Fe_2Os(CO)_{12}]$[34] in the solid state has been examined by ^{13}C CP MAS NMR spectroscopy. In order to interpret solid-state ^{13}C NMR spectra of $[Fe_3(CO)_{12}]$, it has been proposed that the Fe_3 triangle undergoes a 60° rotation about the C_3 axis of the Fe_3 triangle.[12] This proposal arose from applying the Ligand Polyhedral Model without considering the consequences in terms of the Localised

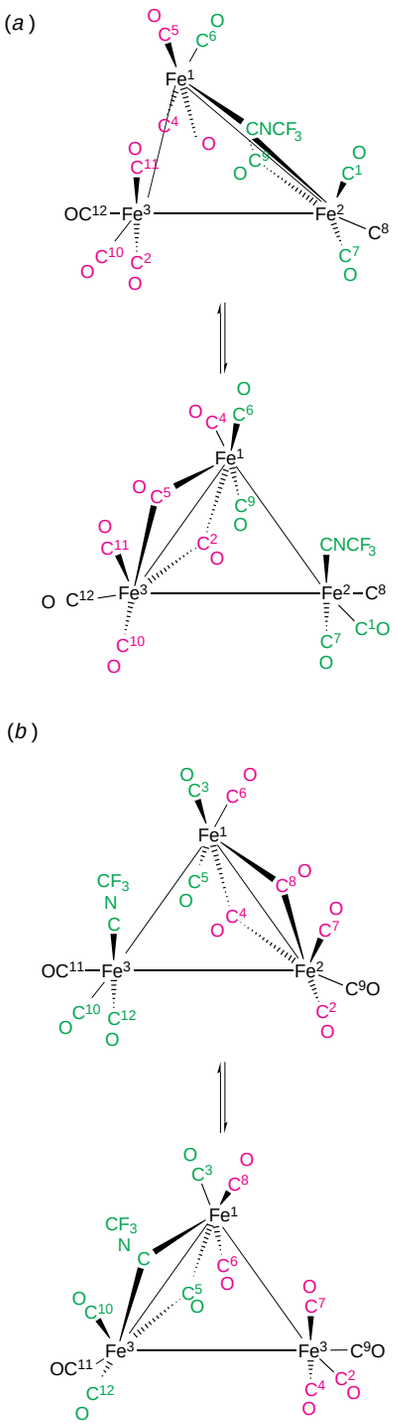

Scheme 10 The concerted-bridge-opening bridge-closing mechanism as applied to $[Fe_3(CO)_{11}(CNCF_3)]$ **8**. (*a*) First there is concerted-bridge-opening on the Fe^2–Fe^3 edge while the bridge closes on the Fe^1–Fe^3 edge. (*b*) There is then concerted-bridge-opening on the Fe^1–Fe^2 edge while the bridge closes on the Fe^1–Fe^3 edge. The resulting exchange is $C^2O \leftrightarrow C^6O \leftrightarrow C^{12}O \leftrightarrow C^9O \leftrightarrow C^5O$ and $C^3O \leftrightarrow C^{10}O \leftrightarrow C^8O \leftrightarrow C^{11}O \leftrightarrow C^7O$

Bonding Model. The mechanism is reproduced in Scheme 11 along with a representation of the intermediate/transition state halfway through the dynamic process. When viewed from the Localised Bonding Model, the intermediate/transition state, **15**, is unprecedented, and the mechanism is implausible.

A more satisfactory explanation is provided by the concerted bridge-opening bridge-closing mechanism. If the carbonyls of $[Fe_3(CO)_{12}]$ move relative to the unit cell of the crystal, then the concerted bridge-opening bridge-closing mechanism about each edge of the iron triangle would result in all the carbonyls averaging. Constraints are applied by the crystal packing, and it can be anticipated that it is easier for the Fe_3 triangle to move

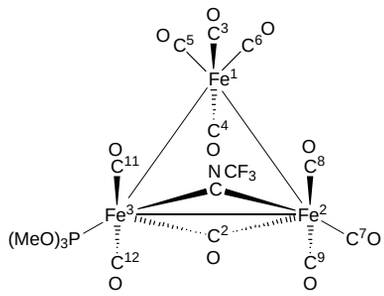

14

within the icosahedron of carbonyls than for the icosahedron of carbonyls to move relative to the neighbouring icosahedra in the crystal. It is known that in solution the barrier to the carbonyl exchange is less than 25 kJ mol^{-1}. This is expected to increase in the solid state. The icosahedron of carbonyls is flattened from the perfect icosahedron by *ca.* 1.5 Å, see Figs. 2(*c*) and 4(*a*). The opposite edges defined by carbonyls C^1O–C^3O and C^2O–C^4O are closer together than for a perfect ligand icosahedron. During the concerted bridge-opening bridge-closing mechanism, as the Fe_3 triangle rotates in 36° steps about the C^6O–$C^{10}O$ axis, the flattening is progressively transferred to edges $C^{11}O$–C^3O and C^9O–C^2O, C^5O–$C^{11}O$ and C^7O–C^9O, $C^{12}O$–C^5O and C^8O–C^7O, C^4O–$C^{12}O$ and C^1O–C^8O, and after five 36° rotations back to the edges C^1O–C^3O and C^2O–C^4O. A rotation of 180° about the C^6O–$C^{10}O$ axis produces approximately the same flattened icosahedron in the crystal lattice as the starting point. The intermediate positions with a 36, 72, 108 and 144° rotation produce a substantial distortion of the pseudo-icosahedron and of the crystal lattice, and are not observed in $[Fe_3(CO)_{12}]$. The crystal structure has disorder between two orientations of the Fe_3 triangle, related by a 180° rotation, to give a 'star-of-David' shape. This led Hanson and co-workers[12] to describe the fluxionality of $[Fe_3(CO)_{12}]$ as arising from a 60° rotation about the C_3 axis through the centre of the Fe_3 triangle. A rotation of 180° about the C^6O–$C^{10}O$ axis produces exactly the same result as the 60° rotation about the C_3 axis through the Fe_3 triangle, but does not involve an unprecedented intermediate/transition state, see Scheme 11. The effect of the 180° rotation about the S_{10} axis through the ligands 6 and 10 is summarised in Scheme 12. This exchanges the carbonyls C^1O, C^2O, C^3O, C^4O; C^5O, C^6O, C^7O, $C^{10}O$; while C^8O, C^9O, $C^{11}O$ and $C^{12}O$ remain unaffected. This is exactly the prediction made by the 60° rotation mechanism in Scheme 11. The multiplicity of ^{13}C NMR signals in the solid state is attributed to crystal packing.

It had been believed that support for the Hanson 60° rotation mechanism had been found in the crystal structure of $[Fe_2Os(CO)_{12}]$, which shows two inter-penetrating triangles, mutually rotated by 180° about the C_3 axis through the metal triangle.[2–4,20] However, the EXSY ^{13}C CP MAS NMR spectrum gave results which were inconsistent with a simple rotation. It was proposed that the mechanism consists of a 60° rotation of the Fe_2Os triangle followed by reorganisation of the carbonyls to return to the ground-state structure. Exactly the same exchange can be achieved by extending Scheme 12, where as with the 60° rotation mechanism, the mechanism puts the osmium onto a bridged edge, and it is necessary to carry out a merry-go-round exchange to put the bridging carbonyl back onto the Fe_2 edge, see Scheme 13. The 180° rotation to move the Fe_2Os triangle to the alternative orientation observed in the crystal structure can be achieved by repeating this two more times.

Comments on the Ligand Polyhedral Model as Applied to $[Fe_3(CO)_{12}]$ and its Derivatives

The Ligand Polyhedral Model is very elegant. It is an alternative way to present an exchange mechanism. Any mechanism which

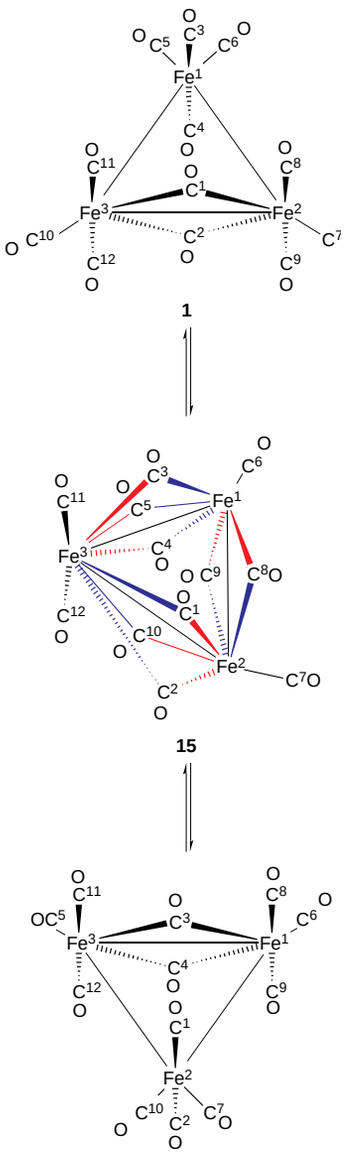

Scheme 11 The application of the rotation of the Fe_3 triangle 60° to the rotation of $[Fe_3(CO)_{12}]$ **1**.[12] Red is used for bonds which are shortening or forming, blue is used for bonds which are lengthening or breaking

can be represented by the Local Bonding Mechanism can also be represented by the Ligand Polyhedral Model and *vice versa*. The Ligand Polyhedral Model has been used in this paper as an equivalent description of the concerted bridge-opening bridge-closing mechanism as an S_{10} rotation of the icosahedron of carbonyls about the axis defined by the ligands in positions 6 and 10.

The Ligand Polyhedral Model has also been applied to the Cotton merry-go-round mechanism in $[Fe_3(CO)_{12}]$ and its derivatives. This mechanism has been supported by the application of the Bürgi–Dunitz analysis and must be viewed as proven beyond reasonable doubt.[18] The choice between the description of the mechanism based on the original Cotton merry-go-round using the Local Bonding Model or the Ligand Polyhedral Model is a matter of personal preference.

The Ligand Polyhedral Model does present traps for the unwary. It is very easy to be seduced by its beauty and to suggest mechanisms which would be untenable using the Local Bonding Model. This is a result of losing sight of the connectivities between the ligands and the metal atoms when using this model. There are several examples of this in the literature.

Johnson and Bott[11] used the C_2 libration mechanism to predict that the carbonyls of $[Fe_3(CO)_{11}(CNBu^t)]$ **11** would be static in CH_2Cl_2 at low temperature. This was because the

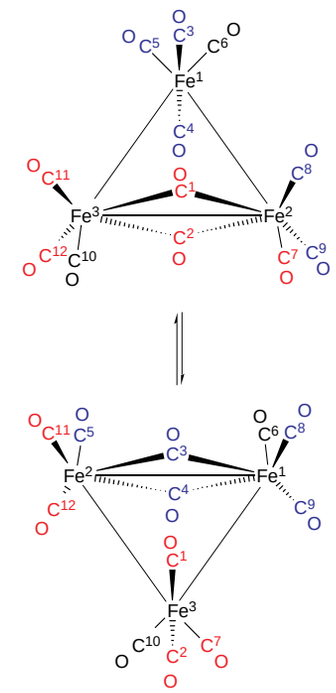

Scheme 12 The effect of rotating the Fe_3 triangle 180° about the pseudo S_{10} axis through C^6O and $C^{10}O$ in $[Fe_3(CO)_{12}]$. The two sets of five carbonyls between which the Fe_3 triangle rotates are identified in red and blue. The carbonyl icosahedron remains approximately fixed

$CNBu^t$ group is in an axial position on the unbridged iron, which they argued will block the libration about the C_2 axis. We have shown that, at −82 °C, $[Fe_3(CO)_{11}(CNBu^t)]$ has three carbonyl signals in the intensity ratio of 1:5:5.[36] This is consistent with the concerted bridge-opening bridge-closing mechanism, see Scheme 3. The fluxionality can readily occur by the $CNBu^t$ group going into the equatorial position as in $[Fe_3(CO)_{10}(CNBu^t)_2]$ **9**[37] or bridging as in $[Fe_2(\eta^5\text{-}C_5H_5)_2(CO)(\mu\text{-}CO)(CNMe)(\mu\text{-}CNMe)]$.[54]

It has been shown in Schemes 9 and 11 how the Ligand Polyhedral Model can conceal improbable intermediates/transition states for the C_5 rotation of the metal triangle about the ligand icosahedral 1–4 axis and for the 60° rotation of the metal triangle about the C_3 axis. These mechanisms have not been disproven, but they are unprecedented and it would have been difficult to persuade the referees and readers to take them seriously if they had been presented using the description of the Local Bonding Model rather than the equivalent Ligand Polyhedral Model.

This demonstrates the major difficulty with the concept of moving the metal cluster within a polyhedron of ligands. It is very easy to lose sight of the relationship between the ligands and the metal cluster. When the fluxionality is viewed using the more familiar Local Bonding Model, the connectivity between the metals and ligands is preserved. It is then easier to see the relationship between the ligands and the metal cluster in both intermediates and transition states, and to compare the predicted structures with ones that are known.

Conclusion

In conclusion, the crystal structure and NMR evidence provide strong support for the concerted bridge-opening bridge-closing mechanism for $[Fe_3(CO)_{12}]$ and its derivatives. The mechanism can equally well be described as an S_{10} rotation about the axis through ligands 6 and 10. The merry-go-round mechanism is generally the next available higher-energy mechanism. The concerted bridge-opening bridge-closing mechanism accounts for the lowest energy dynamic processes in $[Fe_3(CO)_{12}]$ and its derivatives both in solution and in the solid state. Although

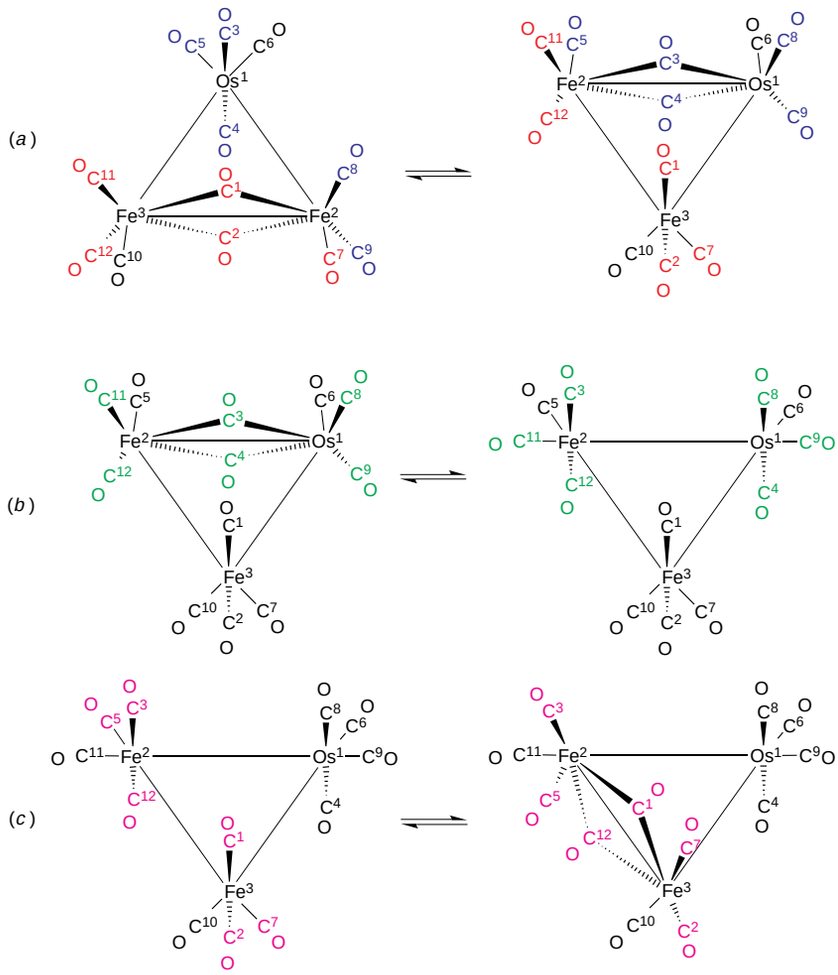

Scheme 13 (*a*) The effect of rotating the Fe_2Os triangle 180° or $^5S_{10}$ about the pseudo S_{10} axis through C^6O and $C^{10}O$ in $[Fe_3(CO)_{12}]$. The two sets of five carbonyls between which the Fe_2Os triangle rotates are identified in red and blue. The carbonyl icosahedron remains approximately fixed. Note that as a result of the rotation the Fe^2–Os^1 edge of the metal triangle becomes bridged. The ground state with the carbonyl bridge on the Fe_2 edge is re-established by the merry-go-round mechanism, with (*b*) the bridge-opening with the moving carbonyls in green and (*c*) the bridge-reclosing onto the Fe_2 edge with the moving carbonyls in magenta

the C_2 libration mechanism produces the same overall ligand exchange as the concerted bridge-opening bridge-closing mechanism, the Bürgi–Dunitz approach clearly shows that the reaction pathway follows the concerted bridge-opening bridge-closing mechanism and not the C_2 libration mechanism. It is shown that both the C_5 rotation mechanism through the ligands 1 and 4 and the C_3 triangle rotation mechanism have implausible intermediates/transition states. The experimental results previously explained using these mechanisms are better explained using the concerted bridge-opening bridge-closing mechanism.

The Ligand Polyhedral Model is very attractive in concept, but is very dangerous to use in practice, having led to several unwise mechanistic suggestions. It is the author's opinion that the Local Bonding Model should be used initially for all mechanistic discussions, and the Ligand Polyhedral Model should only be used subsequently, when necessary, to assist in the description of the mechanism. Either model can be used to describe a given fluxional mechanism. It is a matter of personal preference which model is to be used when a mechanism is presented. However, the reader may wish to compare the Local Bonding Model and the Ligand Polyhedral Model in Schemes 1, 3 and 4 and decide which is more readily understood.

Experimental

The crystal structures described in this paper were downloaded from the Cambridge Crystallographic Database at Daresbury or taken from in-house data.[26,36] The structures were manipulated using CSC Chem3D™ from Cambridge Scientific Computing, Inc., Cambridge, Massachusetts.

Acknowledgements

Thanks are due to the EPSRC for financial support and for access to the Cambridge Crystallographic Data Base. I wish to thank Dr N. A. Bailey for his assistance in helping me to appreciate the crystal packing in $[Fe_3(CO)_{12}]$ and $[Fe_2Os(CO)_{12}]$.

References

1 J. Dewar and H. O. Jones, *Proc. R. Soc. London, Ser. A*, 1906, **76**, 66.
2 C. H. Wei and L. F. Dahl, *J. Am. Chem. Soc.*, 1969, **91**, 1351.
3 F. A. Cotton and J. M. Troup, *J. Am. Chem. Soc.*, 1974, **96**, 4155.
4 D. Braga, F. Grepioni, L. J. Farrugia and B. F. G. Johnson, *J. Chem. Soc., Dalton Trans.*, 1994, 2911.
5 R. K. Sheline, *J. Am. Chem. Soc.*, 1951, **37**, 1615; J. W. Cable and R. K. Sheline, *Chem. Rev.*, 1956, **56**, 1; G. R. Dobson and R. K. Sheline, *Inorg. Chem.*, 1963, **2**, 1313.
6 F. A. Cotton and G. Williamson, *J. Am. Chem. Soc.*, 1957, **79**, 752; K. Noack, *Helv. Chim. Acta*, 1962, **4**, 1847.
7 S. Dobbs, S. Nunziante-Cesaro and M. Maltese, *Inorg. Chim. Acta*, 1986, **113**, 167.
8 F.-W. Grevels, J. Jacke and K. Seevogel, *J. Mol. Struct.*, 1988, **174**, 107.
9 F. A. Cotton, *Inorg. Chem.*, 1966, **5**, 1083.
10 H. Adams, N. A. Bailey, G. W. Bentley and B. E. Mann, *J. Chem. Soc., Dalton Trans.*, 1989, 1831.

11 B. F. G. Johnson and A. Bott, *J. Chem. Soc., Dalton Trans.*, 1990, 2437.
12 (*a*) H. C. Dorn, B. E. Hanson and E. Motell, *Inorg. Chim. Acta*, 1981, **74**, L71; (*b*) B. E. Hanson, E. C. Lisic, J. T. Petty and G. A. Iannaconne, *Inorg. Chem.*, 1986, **25**, 4062; (*c*) J. W. Gleeson and R. W. Vaughan, *J. Chem. Phys.*, 1983, **78**, 5384.
13 D. Lentz and R. Marschall, *Organometallics*, 1991, **10**, 1487.
14 J. Li and K. Jug, *Inorg. Chim. Acta*, 1992, **196**, 89.
15 F. A. Cotton and D. L. Hunter, *Inorg. Chim. Acta*, 1974, **11**, L9.
16 A. Sironi, *Inorg. Chem.*, 1996, **35**, 1725.
17 R. E. Benfield and B. F. G. Johnson, *J. Chem. Soc., Dalton Trans.*, 1978, 1554.
18 R. H. Crabtree and M. Lavin, *Inorg. Chem.*, 1986, **25**, 805.
19 H. B. Bürgi and J. D. Dunitz, *Acc. Chem. Res.*, 1983, **16**, 153; *Structure Correlation*, eds. H. B. Bürgi and J. D. Dunitz, VCH, Weinheim, 1994, vol. 1 and 2, especially T. A. D. Heyde, ch. 8.
20 C. H. Wei and L. F. Dahl, *J. Am. Chem. Soc.*, 1966, **88**, 1821; P. Corradini and G. Paiaro, *Ric. Sci.*, 1966, **36**, 365.
21 R. E. Benfield, P. D. Gavens, B. F. G. Johnson, M. J. Mays, S. Aime, L. Milone and D. Osella, *J. Chem. Soc., Dalton Trans.*, 1981, 1535.
22 B. E. Mann and B. F. Taylor, *^{13}C NMR Data for Organometallic Compounds*, Academic Press, London, 1981.
23 D. H. Farrar and J. A. Lunniss, *J. Chem. Soc., Dalton Trans.*, 1987, 1249.
24 S. Aime, M. Botto, O. Gambino, R. Gobetto and D. Osella, *J. Chem. Soc., Dalton Trans.*, 1989, 1277.
25 B. F. G. Johnson and Y. V. Roberts, *J. Chem. Soc., Dalton Trans.*, 1993, 2945.
26 H. Adams, X. Chen and B. E. Mann, *J. Chem. Soc., Dalton Trans.*, 1996, 2159.
27 I. Brüdgam, H. Hartl and D. Lentz, *Z. Naturforsch., Teil B*, 1984, **39**, 721; D. Lentz, *Z. Naturforsch., Teil B*, 1987, **42**, 839.
28 B. E. Mann, *Organometallics*, 1992, **11**, 481.
29 B. F. G. Johnson, E. Parasini and Y. V. Roberts, *Organometallics*, 1993, **12**, 233.
30 See, for example, Fig. 5 in ref. 11.
31 B. F. G. Johnson, Y. V. Roberts and E. Parisini, *J. Chem. Soc., Dalton Trans.*, 1992, 2573.
32 S. Aime and R. Gobetto, *J. Cluster Sci.*, 1993, **4**, 1.
33 B. F. G. Johnson, *J. Chem. Soc., Chem. Commun.*, 1976, 703.
34 L. J. Farrugia, A. M. Senior, D. Braga, F. Grepioni, A. G. Orpen and J. G. Crossley, *J. Chem. Soc., Dalton Trans.*, 1996, 631.
35 D. J. Dahm and R. A. Jacobsen, *J. Am. Chem. Soc.*, 1968, **90**, 5106.
36 H. Adams, A. G. Carr, B. E. Mann and R. Melling, *Polyhedron*, 1995, **14**, 2771.
37 J. B. Murray, B. K. Nicholson and A. J. Whitton, *J. Organomet. Chem.*, 1990, **385**, 91.
38 R. D. Adams, M. Brice and F. A. Cotton, *J. Am. Chem. Soc.*, 1973, **95**, 6594.
39 R. D. Adams and F. A. Cotton, *J. Am. Chem. Soc.*, 1973, **95**, 6589.
40 M. A. Guillevic, E. L. Hancox and B. E. Mann, *J. Chem. Soc., Dalton Trans.*, 1992, 1729.
41 M. I. Bruce, T. W. Hambley and B. K. Nicholson, *J. Chem. Soc., Dalton Trans.*, 1983, 2385.
42 A. Bino, F. A. Cotton, P. Lahuerta, P. Puebla and R. Usón, *Inorg. Chem.*, 1980, **19**, 2357.
43 F. H. Allen, O. Kennard and R. Taylor, *Acc. Chem. Res.*, 1983, **16**, 146; F. H. Allen, J. E. Davies, J. J. Galloy, O. Johnson, O. Kennard, C. F. Macrae, E. M. Mitchell, G. F. Mitchell, J. M. Smith and D. G. Watson, *J. Chem. Inf. Comput. Sci.*, 1987, **31**, 187.
44 C. J. Cardin, D. J. Cardin, N. B. Kelly, G. A. Lawless and M. B. Power, *J. Organomet. Chem.*, 1988, **341**, 447.
45 G. Ferguson, R. Hourihane and T. R. Spalding, *Acta Crystallogr., Sect. C*, 1991, **47**, 544.
46 T.-J. Kim, S.-C. Kwon, Y.-H. Kim, N. H. Heo, M. M. Teeter and A. Yamano, *J. Organomet. Chem.*, 1991, **426**, 71.
47 P. J. Roberts, B. R. Penfold and J. R. Trotter, *Inorg. Chem.*, 1970, **9**, 2137.
48 G. Raper and W. S. McDonald, *J. Chem. Soc. A*, 1971, 3430.
49 M. I. Bruce, M. J. Liddell, O. bin Shwakataly, C. A. Hughes, B. W. Skelton and A. H. White, *J. Organomet. Chem.*, 1988, **25**, 805.
50 B. E. Mann, M. D. Vargas and R. Khatter, *J. Chem. Soc., Dalton Trans.*, 1992, 1725.
51 F. A. Cotton and D. L. Hunter, *J. Am. Chem. Soc.*, 1976, **98**, 1413.
52 A. J. Campbell, C. E. Cottrell, C. A. Fyfe and K. R. Jeffrey, *Inorg. Chem.*, 1976, **15**, 1321.
53 D. Braga, *Chem. Rev.*, 1992, **92**, 633.
54 F. A. Cotton and B. A. Frenz, *Inorg. Chem.*, 1974, **13**, 253.

Received 18*th June* 1996; *Paper* 6/06981I